Document ID: ECAR-2066
Project No: 23841
Revision No: 0
Effective Date: 10/09/2012

Engineering Calculations and Analysis

ECAR Title: Preliminary JMOCUP As-Run Daily Depletion Calculation for the AGR-2 Experiment in ATR B-12 Position

ECAR No.: 2066

Performer:	J. W. Sterbentz	C110	James W. Sterbentz (Signature)	10/9/2012 (Date)
Checker[1]:	R. L. Sant	C210	(Signature)	10/9/2012 (Date)
Independent Peer Reviewer[2]:			N/A (Signature)	(Date)
CUI Reviewer: Yes ____ or No[5] _X_			N/A (Signature)	(Date)
Manager[3]:	D. A. Petti	C020	David Petti (Signature)	10/9/2012 (Date)
Owner[4]:	D. A. Petti	C020	David Petti (Signature)	10/9/2012 (Date)
Nuclear Safety[4]:			N/A (Signature)	(Date)
Cognizant Engineer[4]:			N/A (Signature)	(Date)
Quality Assurance:	D. R. Jensen	Q580	(Signature)	10/9/12 (Date)

1. Confirmation of completeness, mathematical accuracy, and correctness of data and appropriateness of assumptions.
2. Concurrence of method or approach. See definition, LWP-10106.
3. Concurrence of procedure compliance. Concurrence with method/approach and conclusion.
4. Concurrence with the document's assumptions and input information. See definition of Acceptance, LWP-10200.
5. Does the document contain CUI material please check either yes or no.

Title: Preliminary JMOCUP As-Run Daily Depletion Calculation for the AGR-2 Experiment in ATR B-12 Position

ECAR No.: 2066 Rev. No.: 0 Project No.: 23843 Date: 10/09/2012

REVISION LOG

Rev.	Date	Affected Pages	Revision Description
0	10/09/2012	All	New Document

Title: Preliminary JMOCUP As-Run Daily Depletion Calculation for the AGR-2 Experiment in ATR B-12 Position

ECAR No.: 2066 Rev. No.: 0 Project No.: 23843 Date: 10/09/2012

1. Quality Level (QL) No.	QL-2	**Professional Engineer's Stamp** See LWP-10010 for requirements.
2. QL Determination No.	REC-000169	
3. Engineering Job (EJ) No.	NA	
4. SSC ID	NA	
5. Building	NA	
6. Site Area	NA	

7. Objective/Purpose:
The objective of this analysis was to perform a high-resolution or daily as-run physics depletion analysis for the Advanced Gas Reactor-2 (AGR-2) tristructural-isotropic (TRISO) particle fuel experiment in B-12 test facility of the Advanced Test Reactor (ATR). Since the AGR-2 experiment has currently only completed eight of the 13 projected ATR power cycle irradiations, this Engineering Calculations and Analysis Report (ECAR) (Rev. 0) is intended as an interim progress status of calculated physics data. Preliminary physics data presented here includes estimates for compact burnup (%FIMA), compact fast fluence (>0.18 MeV), compact actinide isotopic concentration as a function of burnup, compact actinide isotopic specific fissions as function of burnup, and depletion characteristics for the ATR core, borated graphite holders, and hafnium shroud.

Future revisions of this ECAR shall include updates to the above calculated physics data, plus the following that are not included in this revision:

1) Compact fission heat rates (W/cm^3) on a daily basis for each ATR power cycle

2) Compact I-135 concentrations at the end of each ATR power cycle with no decay

3) Compact actinide and fission product concentrations at the end of the AGR-2 irradiation.

The AGR-2 JMOCUP depletion analysis was performed using the computer codes MCNP5 and ORIGEN2.2 coupled through the JMOCUP processing modules. A description of the JMOCUP depletion analysis and verification of the computer software can be found in Reference 1 (ECAR-958, Rev.1).

8. If revision, please state the reason and list sections and/or pages being affected:

9. Conclusions/Recommendations:

The JMOCUP Monte Carlo depletion methodology has been applied to the AGR-2 TRISO coated fuel particle irradiation test in the B-12 position in the ATR. The JMOCUP depletion calculations at present include only the first eight ATR power cycles of the AGR-2 test and the calculated results herein are only for these first eight cycles. There are five more ATR power cycle irradiations expected before the AGR-2 test is done. Selected calculated results are presented herein.

As part of the quality assurance (QA) process, the AGR-2 MCNP model underwent an independent technical check. The JMOCUP modules were previously verified during the AGR-1 JMOCUP depletion calculation [1] and are used in the AGR-2 calculations with minor modifications that have been verified.

CONTENTS

APPENDIXES

Title: Preliminary JMOCUP As-Run Daily Depletion Calculation for the AGR-2 Experiment in ATR B-12 Position

ECAR No.: 2066 Rev. No.: 0 Project No.: 23843 Date: 10/09/2012

PROJECT ROLES AND RESPONSIBILITIES

Project Role	Name (Typed)	Organization	Pages covered (if applicable)
Performer	J. W. Sterbentz	C110	
Checker[a]	R. L. Sant	C210	
Independent Reviewer[b]	None		
CUI Reviewer[c]			
Manager[d]	G. J. Youinou	C110	
Requestor[e]	J. T. Maki	C620	
Nuclear Safety[e]			
Document Owner[e]			
VHTR TDO Manager	D. A. Petti	C020	
Quality Assurance	D. R. Jensen	Q580	

Responsibilities:

a. Confirmation of completeness, mathematical accuracy, and correctness of data and appropriateness of assumptions.

b. Concurrence of method or approach. See definition, LWP-10106.

c. Concurrence with the document's markings in accordance with LWP-11202.

d. Concurrence of procedure compliance. Concurrence with method/approach and conclusion.

e. Concurrence with the document's assumptions and input information. See definition of Acceptance, LWP-10200.

NOTE: *Delete or mark "N/A" for project roles not engaged. Include ALL personnel and their roles listed above in the eCR system. The list of the roles above is not all inclusive. If needed, the list can be extended or reduced.*

1. INTRODUCTION

This report is intended to document the physics depletion calculations for the Advanced Gas Reactor experiment number 2 (AGR-2) located in the B-12 position of the Advanced Test Reactor (ATR). The AGR-2 calculations here use the same JMOCUP Monte Carlo depletion methodology and software modules previously used in the AGR-1 physics calculations.

The JMOCUP physics calculation applied to the AGR-2 attempts to fully simulate the ATR reactor under as-run operating conditions and specifically during those power cycles in which the AGR-2 experiment was in the ATR undergoing irradiation. In the calculations, the ATR driver core is depleted simultaneously along with AGR-2 experiment components which include the TRISO particle fuel compacts, the borated graphite holders, and hafnium shroud. The depletion calculations use relatively short time steps (24-hours or daily timesteps) to achieve relatively high resolution for specific AGR-2 physics parameters.

In general, reactor core depletion calculations do not require daily time steps to achieve desired computational accuracy for burnup estimates. The main reason for the daily timestep here was to achieve high-resolution heat rate estimates for the AGR-2 experiment components. The calculated daily component heat rate estimates together with measured daily helium-neon gas mixtures are then used as input in the thermal analysis model. The thermal model is used to predict temperatures throughout the AGR-2 test train assembly, but primarily for estimating daily tristructural-isotropic (TRISO) particle compact temperatures and comparing calculated thermocouple temperatures to the measured thermocouple temperatures (TCs are placed throughout the graphite holders in each capsule).

The physics model accounts for the daily changes or fluctuations in the ATR core power and lobe power, outer shim control cylinders (OSCC) movements, neck shim withdrawals, and ATR driver fuel burnup. By comparing the calculated temperatures with the actual thermocouple temperature measurements, the thermocouple performance and drift could be assessed. Temperature is an important variable for understanding the time-dependent irradiation behavior and performance of the TRISO coated fuel particles.

The relatively large number of timesteps (daily) requires significant computer resources in terms of computing power, speed, and disk space storage in order to complete the calculations in a reasonable amount of time. In addition, at the beginning of each timestep, the JMOCUP simulation adjusts the ATR OSCC and the neck shim rods appropriately using the as-run measured ATR surveillance data to achieve and maintain a near-critical ATR core configuration.

In addition to the daily (24-hour) time step subdivision of each ATR power cycle, some time steps were less than 24 hours. Shorter time steps were required for transient operating conditions that included beginning-of-cycle (BOC) power ramp-up, scrams, power ramp-up from a scram, and end-of-cycle (EOC) shutdown. Some additional short times were also used to line up with the data acquisition times of the helium-neon gas control system.

The daily depletion time steps do account for the continuous adjustment of the outer shim control cylinders during reactor operation. The AGR-2 test capsule was in the B-12 test location, which is sandwiched between two OSCCs (W2 and W3). Rotational movement of these two cylinders can significantly impact the magnitude of the thermal neutron flux in the B-12 test facility [1] and, hence, the fuel compact fission powers. The greatest impact or increase to the thermal flux in a large-B position, such as the boron-10, is near the end of some ATR power cycles when the OSCCs are turned way out.

For example, a 62% increase in the thermal neutron flux is possible for OSCC rotations starting at 85° and ending at 110°.

Some of the 8 AGR-2 ATR power cycles experience large-angle OSCC rotations near end-of-cycle. The impact of these large-angle EOC rotations is evident relative to the calculated capsule-power and thermocouple-temperature measurements. Therefore, inclusion of the OSCC rotations in the JMOCUP depletion calculation was needed in order to capture this important effect on the compact fission powers.

Subdividing each ATR power cycle into 24-hour increments leads to a relatively large number of time steps per power cycle. This drives the JMOCUP depletion calculation to be a computationally intensive calculation. Table 1 lists the eight ATR power cycles (completed to date) along with the number of time steps per cycle, number of MCNP KCODE calculations, and the number of ORIGEN calculations.

Table 1. Current AGR-2 JMOCUP depletion cycles run and calculational parameters.

No. of ATR Cycles	ATR Cycle	No. Time steps per cycle	Calendar Days at Power	Ave Core Power (MW)	Shutdown Time* (days)
1	147A	54	50.68	108.00	17.4
2	148A	51	47.89	103.77	25.2
3	148B	53	51.81	105.09	95.9
4	149A	38	37.05	106.12	16.2
5	149B	55	53.83	105.58	33.6
6	150B	44	42.42	106.89	17.6
7	151A	59	56.65	100.77	18.8
8	151B	57	51.80	100.46	90.6
9	—	—	—	—	—
10	—	—	—	—	—
11	—	—	—	—	—
12	—	—	—	—	—
13	—	—	—	—	—
Total					

* Shutdown or decay time between cycles

It should be noted that Cycle 150A is missing from Table 1. The AGR-2 experiment was not in the ATR during this PALM cycle, and therefore sustained no burnup from this cycle.

One important feature of the JMOCUP depletion calculation is that it is automated. Once the cycle depletion calculation is set up, and the START button pushed, the JMOCUP modules and scripts control the depletion calculation from the beginning to the end of the cycle without user assistance. The modules read and write data, and the scripts control execution of the codes and direct file inputs and outputs to appropriate directories for later data reduction and evaluation. Large debug output files are also written to allow the user to monitor the calculation processes and check calculated data. The JMOCUP calculation produces massive amounts of output data and, for this reason, many post processing modules have been built to read the thousands of output files and extract data. Plotting these data provides desired calculated results as well as a variety of output data that can be used to help verify the JMOCUP calculation.

However, the JMOCUP depletion calculation does require substantial input data preparation at the beginning of each cycle. ATR surveillance data, such as the total core power, lobe powers, OSCC positions, and neck shim withdrawals, along with the beginning-of-cycle ATR driver fuel-element loadings, all need to be preprocessed, formatted, and loaded into the appropriate JMOCUP modules by the user. Pre-assessment of the as-run data also requires the user to determine the break points for the time steps and, ultimately, the total number of time step subdivisions for each cycle.

This report documents the JMOCUP depletion calculation assumptions, limitations, methodology, models, calculated results, and conclusions as applied to the AGR-2 experiment in the ATR B-12 test position.

2. ASSUMPTIONS

The assumptions used in the JMOCUP depletion calculations and analyses include the following:

- ATR measured data used as input data for the JMOCUP depletion calculation included the hourly ATR total core power, five lobe powers, 16 outer shim control cylinder positions, and 24 neck shim positions for the first 8 AGR-2 ATR power cycles. These ATR power and control history data were obtained directly from the Nuclear Data Management and Analysis System (NDMAS). The NDMAS data come directly from the ATR Surveillance Data System (ASUDAS) reports in real time. The NDMAS has been verified and validated.

- Input data for the JMOCUP depletion calculation also included the initial ATR driver core fuel loadings (U-235 uranium and B-10 loadings by element and position in the core). These data were extracted from the following references:

  a) P. A. Roth, ECAR-1032, Rev. 0, “Results of Reactor Physics Safety Analysis for Advanced Test Reactor (ATR) Cycle 147A, June 01, 2010.

  b) A. W. LaPorta, ECAR-1158, Rev. 0, “Results of Reactor Physics Safety Analysis for Advanced Test Reactor (ATR) Cycle 148A, August 18, 2010.

  c) P. A. Roth, ECAR-1253, Rev. 0, “Results of Reactor Physics Safety Analysis for Advanced Test Reactor (ATR) Cycle 148B, November 02, 2010.

  d) P. A. Roth, ECAR-1408, Rev. 0, “Results of Reactor Physics Safety Analysis for Advanced Test Reactor (ATR) Cycle 149A, February 28, 2011.

  e) P. A. Roth, ECAR-1524, Rev. 0, “Results of Reactor Physics Safety Analysis for Advanced Test Reactor (ATR) Cycle 149B, May 26, 2011.

f) A. W. LaPorta, ECAR-1660, Rev. 0, “Results of Reactor Physics Safety Analysis for Advanced Test Reactor (ATR) Cycle 150B, August 30, 2011.

g) B. J. Curnutt, ECAR-1742, Rev. 1, “Results of Reactor Physics Safety Analysis for Advanced Test Reactor (ATR) Cycle 151A, December 8, 2011.

h) P. A. Roth, ECAR-1804, Rev. 1, “Results of Reactor Physics Safety Analysis for Advanced Test Reactor (ATR) Cycle 151B, February 21, 2012.

i) (to be added at a later date).

j) (to be added at a later date).

k) (to be added at a later date).

l) (to be added at a later date).

m) (to be added at a later date).

- The MCNP base model used in the JMOCUP AGR-2 calculations is based on the AGR-1 JMOCUP calculation [1]. The heat rate calculations use this MCNP base model with the TRISO particle compacts homogenized and the compacts divided into two axial cells for better resolution needed in the thermal model calculation. All other calculated physics data is based on this same MCNP base model but with the TRISO particles explicitly modeled; the physics data is typically averaged over a compact.

- In the homogenized compact model, the fuel compact materials are homogenized, which means the TRISO particles and graphite binder matrix materials are assumed to be uniformly mixed.

- In the particle model, explicit particles are modeled based on fuel type (capsule) with appropriate kernel and coating dimensions and material densities.

- Neutron cross-section data in the base MCNP model of the ATR are primarily ENDF-6, plus some ENDF-5 cross-section data for certain fission products and natural elements. Compact actinide cross sections are based on ENDF-6 data. All the fission products in the compacts and Am-242m were from the ENDF-7 cross-section library data.

- High-temperature neutron cross-section data for actinides and fission products in the compacts were generated using both ENDF-6 data at room temperature. High-temperature cross sections for all the fission products and Am-242m were generated using ENDF-7 data.

- The west-lobe source power is defined as the average of the NW, C, and SW lobe powers, W = (NW + C + SW)/3 and is used to normalize powers and fluxes in the B-12 test facility.

- Beginning-of-cycle (BOC) refers to the start of an ATR power cycle; end-of-cycle (EOC) refers to the end of an ATR power cycle.

- Beginning of life (BOL) refers to the beginning of the first AGR-2 ATR power cycle (147A); End of life (EOL) refers to the end of reactor operation following the final ATR power cycle for the AGR-2 irradiation test.

3. AGR-2 EXPERIMENT ASSEMBLY

The AGR-2 test train assembly was irradiated in the ATR B-12 test facility (Figure 1). The test train assembly consisted of six capsules stacked vertically end-to-end (Figure 2). Capsule 1 was at the bottom of the test train assembly, and Capsule 6, at the top. Four different types of TRISO particle fuel are in these six capsules. Capsules 2, 5, and 6 contain compacts with UCO kernel particles fabricated by the United States, while Capsule 3 contains compacts with UO_2 kernel particles fabricated by the United States, Capsule 4 contains compacts with UO_2 kernel particles fabricated by South Africa, and Capsule 1 contains compacts with UO_2 kernel particles fabricated by France. Compact and particle information associated with Capsules 4 and 1 is proprietary. Table 2 lists selected characteristics of the UCO and UO_2 fuel fabricated by the United States [3].

Table 2. Nominal AGR-2 TRISO particle compact characteristics for United States (U.S.) fabricated particles/compacts.

Parameter	UCO Fuel	UO_2 Fuel
Enrichment	14.0 wt%	9.6 wt%
Packing Fraction	36%	23%
Kernel Diameter	427 μm	508 μm
Matrix Density	1.59 g/cm^3	1.68 g/cm^3

Each capsule contained a borated graphite holder. Each borated graphite holder had three equally spaced bore holes to hold three stacks of compacts. Figure 3 shows the three stacks (green) labeled 1, 2, and 3. Note: Stacks 1 and 2 face toward the ATR core center. Each of the three compact stacks per capsule contained four compacts; each compact had a measured average length of approximately 0.99-inch (2.52 cm) length and a diameter of 0.484 inch (1.23 cm) per INL/PLN-3798, “AGR-2 Irradiation Experiment Test Plan” [3].

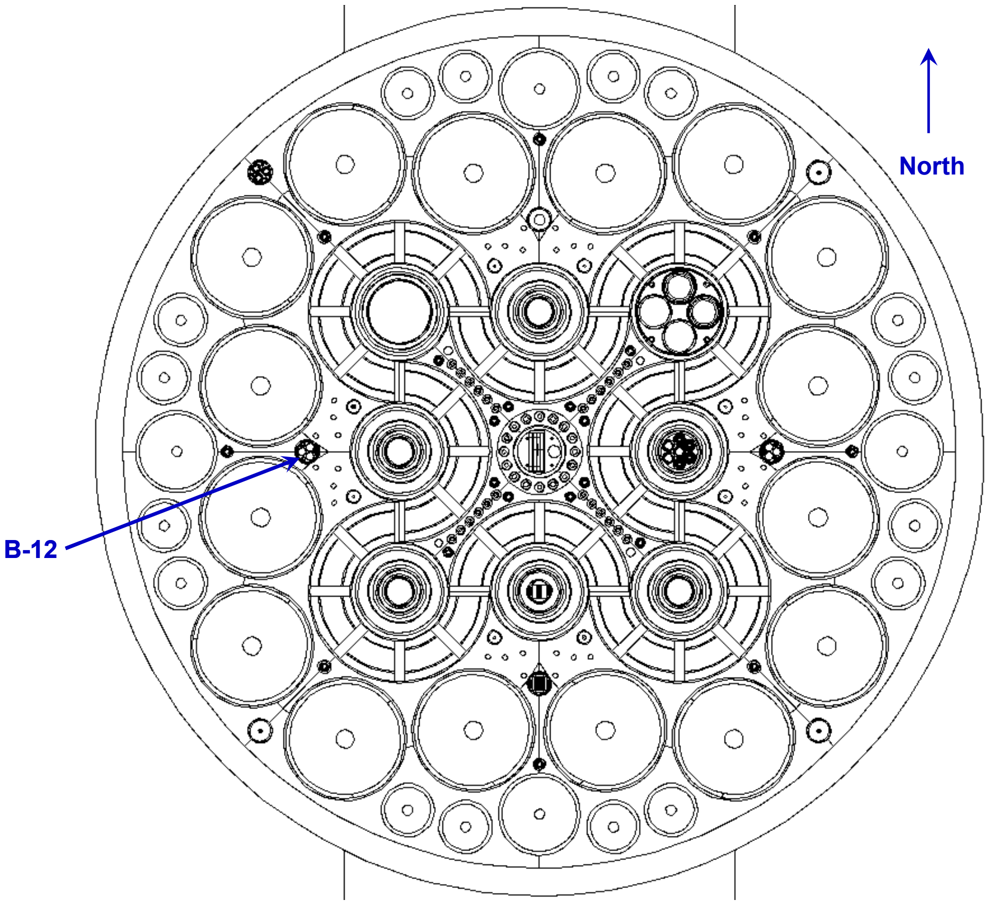

Figure 1. Cross-section view of the ATR core and the B-12 irradiation test facility.

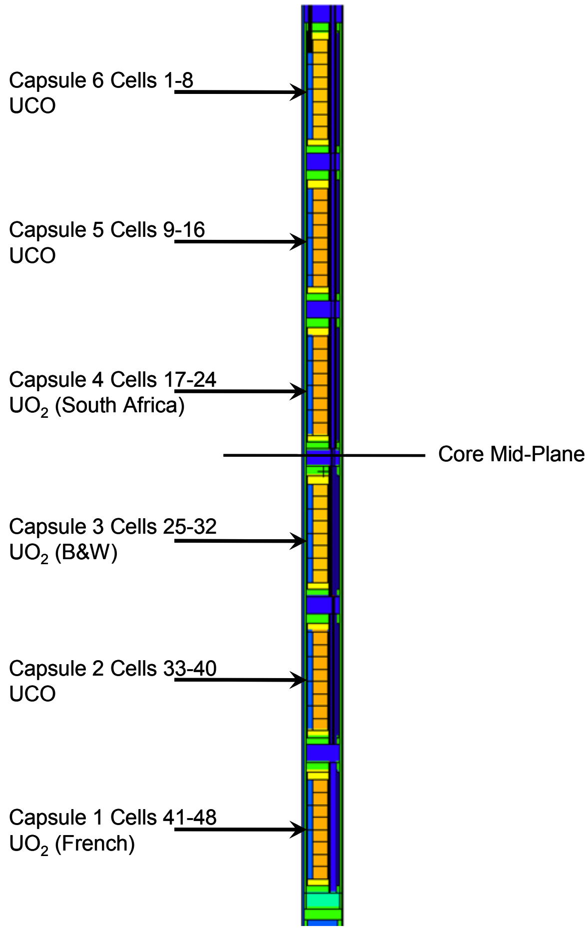

Figure 2. Axial view of the AGR-2 test train assembly, showing the six capsules and details of one of the fuel compact stacks (homogenized model).

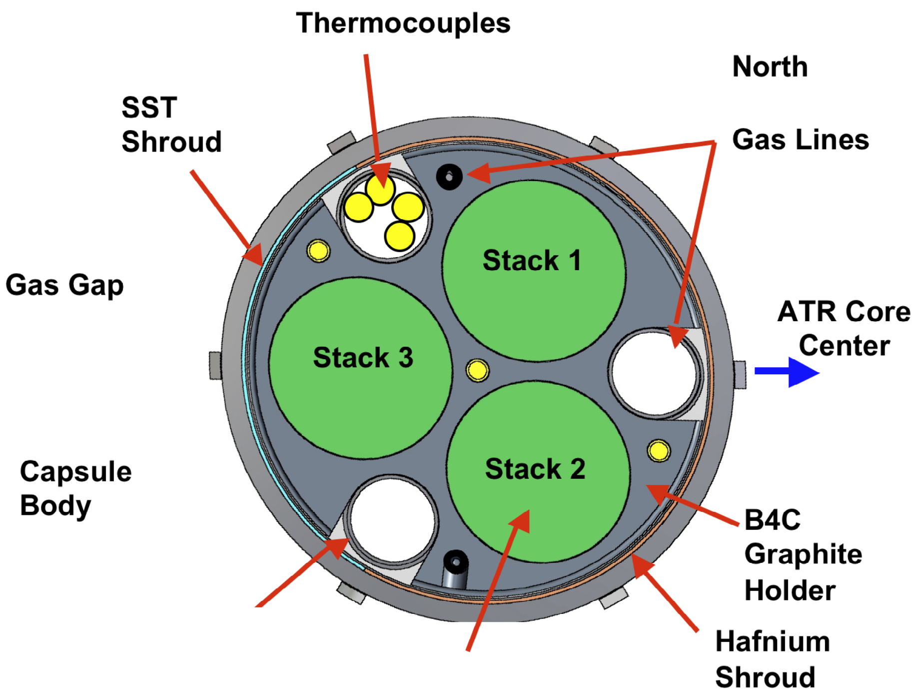

Figure 3. Cross-section view of an AGR-2 capsule.

4. COMPUTER CODES

The following computer codes were used in the AGR-2 JMOCUP depletion calculation:

- The MCNP (Monte Carlo N-Particle) code [4], Version 5, or MCNP5, is a general purpose, continuous energy, generalized geometry, coupled neutron-photon-electron Monte Carlo transport computer code. The powerful geometry capability allows for fully-explicit three-dimensional cell representations of nuclear-reactor core components and geometrical features. The code can be used to calculate a variety of different reactor-physics parameters that include neutron flux, neutron spectra, nuclear reaction rates, fission powers, gamma and neutron heating rates, and core eigenvalues (k-effectives). The MCNP code uses continuous-energy neutron cross sections spanning the energy range from 1.0E-10 to 20.0 MeV for a wide range of natural elements and isotopes; the photon cross-section energy range is from 1 keV to 100 MeV. Cross-section data libraries used in the ATR MCNP full core model for the JMOCUP AGR-2 depletion calculation are mostly from the ENDF-6 or Evaluated Nuclear Data Files Version 6 (endf60), but some cross-section data also comes from ENDF-5.

- The ORIGEN2.2 (Oak Ridge Isotope Generation) code [5], Version 2.2, is used to calculate the time-dependent, coupled behavior of radioactive and stable-isotope buildup, depletion, and decay under constant power or flux conditions. For the AGR-2 JMOCUP depletion calculation, the constant irradiation power option is used for the ATR driver fuel and the constant irradiation flux option is used for the compact, borated graphite holder, and hafnium shroud depletions. Isotope production and destruction mechanisms include transmutation or neutron radiative capture, fission, threshold particle reactions, and radioactive decay processes. The mathematical basis of the ORIGEN2.2 code is the matrix exponential method, which accurately solves the coupled ordinary differential equations relating the isotope reaction and decay mechanisms.

- The JMOCUP code system is a Monte Carlo depletion methodology, which is functionally similar to the MOCUP (MCNP-ORIGEN2 Coupled Utility Program) code system [6]. JMOCUP (or Jim Sterbentz's MOCUP) and MOCUP are both systems of external processors or modules that link the input and output files of MCNP5 and ORIGEN2.2. No modifications to either MCNP5 or ORIGEN2.2 are required to run either JMOCUP or MOCUP. MOCUP is written in C+ and JMOCUP is written in FORTRAN. FORTRAN was the language of choice for JMOCUP since execution speed is not a limiting factor and a GUI interface was not needed nor desired for the computer-intensive and repetitive AGR-2 JMOCUP depletion calculations. Both JMOCUP and MOCUP perform time-dependent depletion calculations in discrete time steps.

- The DOPPLER code [7] allows a user to prepare customized temperature dependent nuclear data files for use with the MCNP5 computer code. The user does not have to then go through the laborious task of processing ENDF data files through the NJOY code to generate new temperature-dependent cross sections. Instead, existing point-wise MCNP cross-section files in ACE format can be broadened to the desired temperature quickly and easily using methods identical to those used for the original preparation of the base data files with the NJOY Nuclear Data Processing System. Thermal-scattering tables and unresolved resonance-range probability tables are interpolated between tables for temperatures surrounding the desired value. This gives the MCNP user a simple but accurate way to prepare nuclear data libraries that exactly match the conditions of the problem being analyzed.

- The NJOY code [7] allows a user to prepare MCNP ACER cross section libraries from the Evaluated Nuclear Data Files (ENDF).

5. ATR/AGR-2 MCNP MODEL

The AGR-2 MCNP model used in the AGR-2 JMOCUP depletion calculations is based on the combination of two verified MCNP models. The first piece is from the previously verified AGR-1 JMOCUP MCNP base model [1] and includes everything in the ATR core except the AGR-2 experiment. The second piece is the collection of MCNP cells that compose the AGR-2 experiment taken from the verified and validated MCNP model from INL/ECAR-949, “Reactor Physics Analysis for the AGR-2 Experiment Irradiated in the ATR B-12 Position” [8]. The AGR-2 MCNP experiment cells from INL/ECAR-949 [8] were basically spliced into the existing AGR-1 JMOCUP base model. Hence, all the information in INL/ECAR-949 [8] will apply to the new AGR-2 MCNP JMOCUP models as well with exceptions noted below.

The AGR-2 MCNP cells from INL/ECAR-949 [8] that were spliced into the new AGR-2 MCNP JMOCUP model include use the TRISO particle characteristics [3], for example, dimensions, enrichment, number of particles per compact, uranium mass loading per compact, calculated number densities, and coating and matrix material densities. Insignificant differences include re-numbering of the MCNP cell and material cards. Correct incorporation of the compact/particle data has been re-verified by an independent checker (Appendix D). Also, the new AGR-2 MCNP JMOCUP model has the AGR-1 experiment removed from the B-10 position and the AGR-2 experiment loaded into the B-12 position.

Further development of the new AGR-2 JMOCUP MCNP model has lead to both a homogenized compact model (***inp.1***) and an explicit particle model (***inq.1***). The homogenized compact model smears the particle kernel and coatings number densities with the graphite matrix binder number density into a single homogenized material. The compacts are further subdivided into two axial cells of approximately 0.5 inch. The homogenized model was used primarily to generate the compact heat rates and the associated capsule component heat rates for use in the thermal analysis model. The explicit particle model modeled individual particles in each compact. The number of particles per compact varied from approximately 1200 to 3200 depending on the four different TRISO particle fuel types in the six capsules. Calculations with the particle model allowed for the self-shielding of the U-238 in the kernels and are expected to produce more accurate plutonium isotopic concentrations along with more accurate uranium and other actinide concentrations, and fission product concentrations too. The particle model produced calculated data averaged over a compact. Compact heat rates calculated with both the homogenized and particle models were very close. However, the homogenized model heat rates were used in the thermal model because of the higher axial resolution in the MCNP compact cells; compacts in the homogenized model were subdivided into two equal volume axial cells, whereas the particle model did not axially subdivide the compacts. The higher axial heat rate resolution from the homogenized model resulted in significantly better axial temperature profiles in the thermal analysis.

Figures 4 and 5 are plots of the ATR/AGR-2 MCNP particle model geometry as plotted by the MCNP code plotter. Specifically, these plots show the regular arrays of UCO (U.S.) particles in both the axial and cross-sectional views. Each axial particle layer has 113 particles per layer and 28 layers per compact.

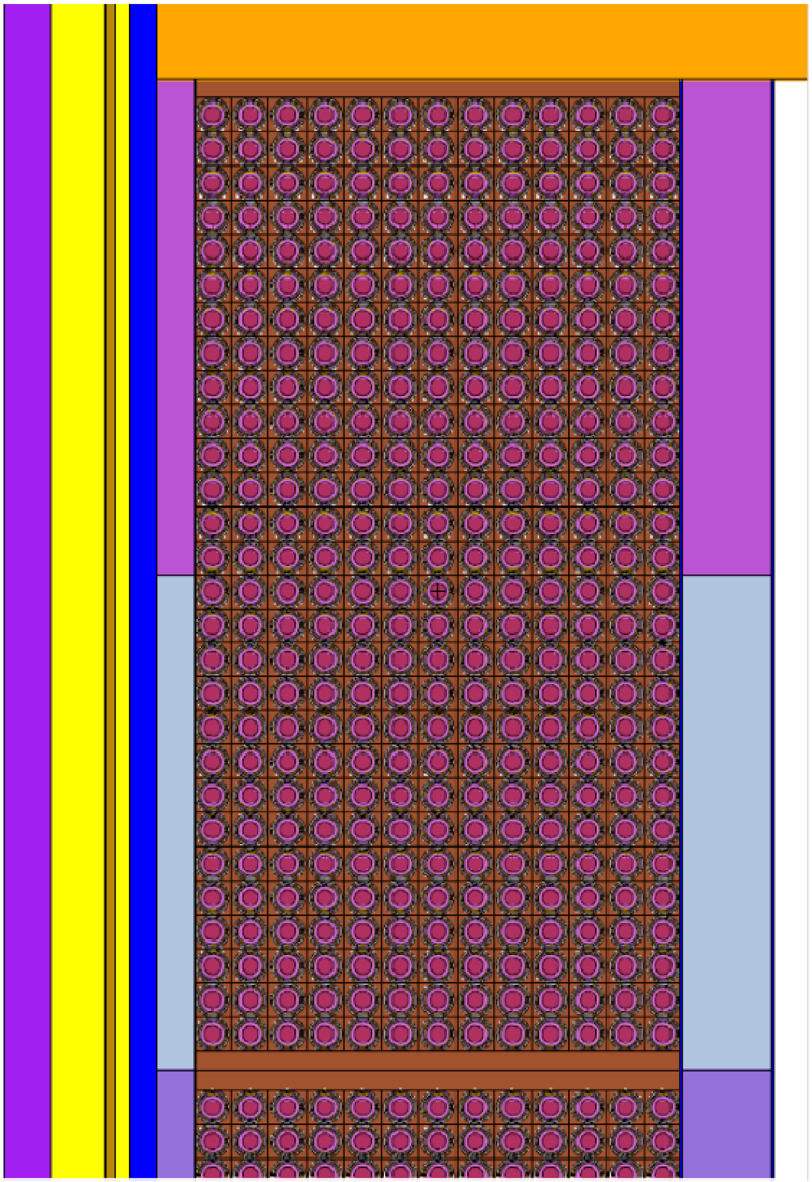

Figure 4. Axial view of the TRISO-coated particles in a UCO (U.S) compact (AGR-2 Capsule 6). Note the 28 particle layers per compact.

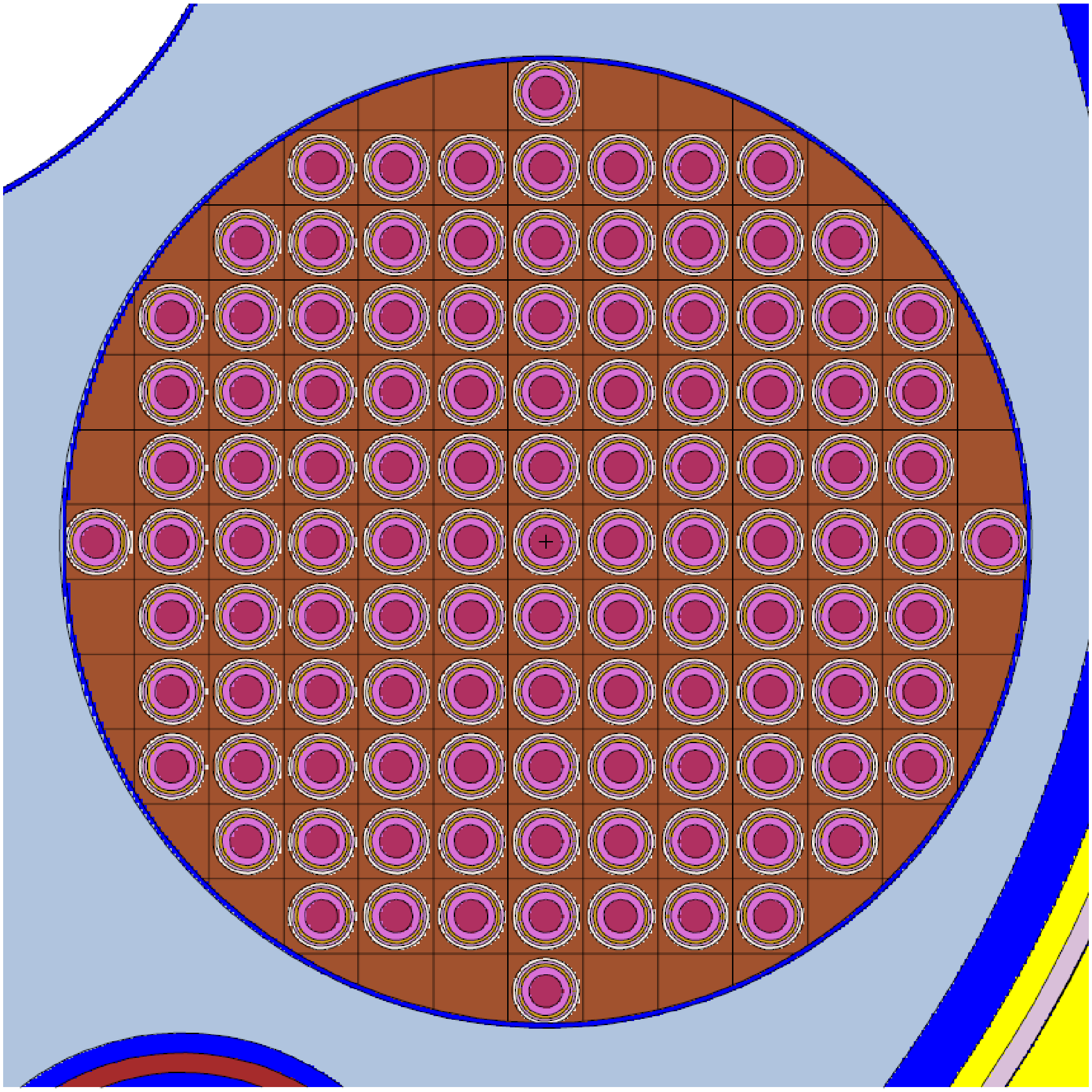

Figure 5. Cross-sectional view of the TRISO coated-particles in a UCO (U.S) compact (AGR-2 Capsule 6). Note the 113 particles per layer.

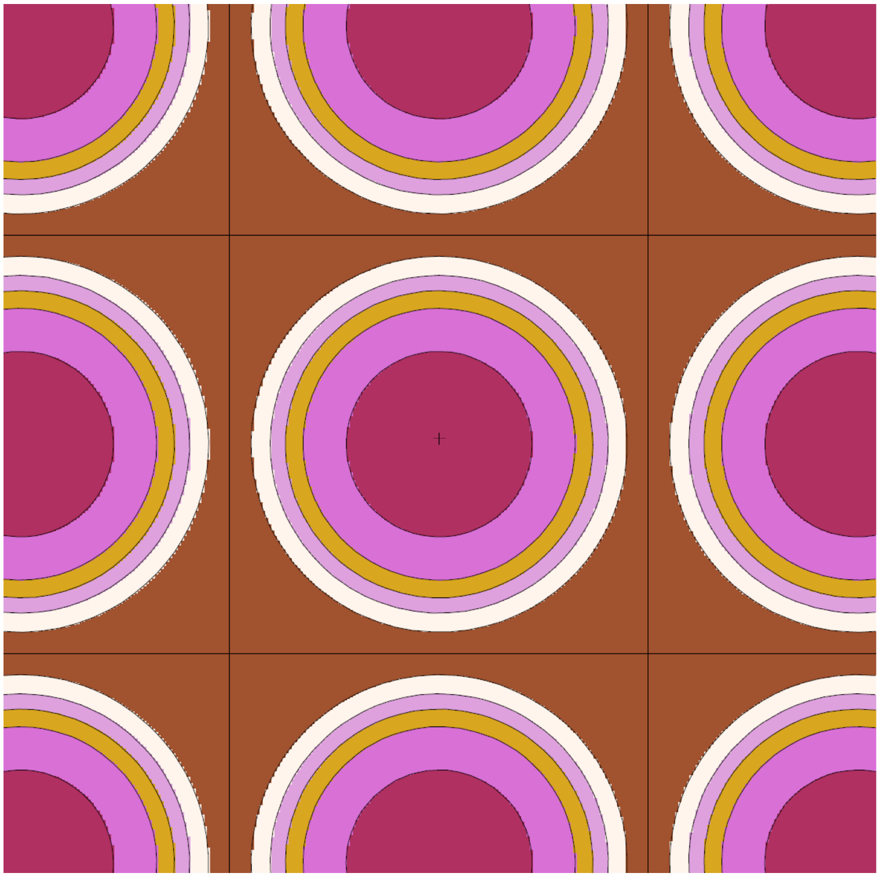

Figure 5a. Close-up of individual TRISO coated-particles showing the UCO kernel, buffer layer, inner pyrolytic graphite layer, silicon carbide pressure vessel layer, and the outer pyrolytic graphite layer.

At the beginning of each new time step, the MCNP base model (***inp.1* and *inq.1***) receives several updates to produce the next MCNP model (***inp.2* and *inq.2***) for the next time step. These updates include:

- ATR driver fuel cell cards total number density
- Material card number density updates for the ATR driver fuel cells, compact cells, hafnium shroud cells, and the borated graphite holder cells
- OSCC surface card changes to reflect the new positions
- Neck shim cell card changes to reflect withdrawals.

The typical JMOCUP MCNP model is approximately 65,000–70,000 lines long and requires approximately 1.5–2.0 hours of execution time on the QUARK computer system with 120 CPUs. The KCODE option used ~7,000,000 starting neutrons/cycle, ~150 cycles, and six skipped or inactive cycles.

The primary neutron cross-section library data used in the MCNP model and transport calculations was from ENDF-VI-2 (endf60). Special temperature dependent cross sections were also developed using the DOPPLER code [7] for the compacts (600 and 1200°C). Fission-product cross-sections libraries were selected from ENDF-V, VI.2, and VII.0. Since none of the fission product libraries contain resonance parameter data, temperature broadening of the resonances had no effect.

6. JMOCUP METHODOLOGY

The JMOCUP depletion methodology was used to perform the AGR-2 fuel compact depletions. Use of the JMOCUP code/module system was previously used for the analysis of the AGR-1 experiment. The complexity of the AGR-2 calculation is comparable to the AGR-1 calculation and despite massive number-crunching operations associated with both the AGR-2 and AGR-1 JMOCUP depletion calculations, the JMOCUP calculation appears to have performed well for the AGR-2 calculation here. Verification of the JMOCUP module operation and performance was performed previously for the AGR-1 calculation [1] and is not repeated here for AGR-2 as the same modules are used. However, the MCNP base models, namely the homogenized model (***inp.1***) and the particle model (***inq.1***), were checked by an independent technical checker. Validation of the JMOCUP depletion calculation will be performed through comparisons of calculated results and post-irradiation examination (PIE) measurement data. Comparisons may include compact/particle U-235 burnup and selected actinide and fission-product concentrations (both absolute and relative).

The AGR-2 JMOCUP depletion calculation coordinated four depletions: (1) ATR driver core, (2) AGR-2 compacts, (3) AGR-2 hafnium capsule shroud, and (4) AGR-2 borated graphite holder. The ATR driver core consists of 840 depletion cells in the MCNP model; 3 radial and 7 axial zones (cells) per element (or 3x7x40=840 depletion cells total). The TRISO particle compacts were depleted using 144 depletion cells in the homogenized model and 72 cells in the particle model. The hafnium shroud had a total of 24 depletion cells and the borated graphite holder a total of 23 depletion cells. Therefore, there are 1,031 and 959 depletion cells in the homogenized and particle models, respectively. JMOCUP depleted each cell at each time step.

The ATR driver depletion cells each contain nine actinides and 24 fission-product isotopes. These 23 isotopes that are tracked meaning that their fission and radiative capture cross sections are updated every time step. Similarly, the compacts have 19 tracked actinides and 71 fission products. In the hafnium shroud cells, the six naturally occurring hafnium isotopes are tracked, as is the boron-10 in the 23 borated graphite cells that compose the AGR-2 graphite compact holder. The MCNP code calculates the cell neutron flux and nuclear reaction rate(s) for every isotope in each depletion cell at every time step. Using these data, updated one-group cross sections are fed to the ORIGEN input files for the next ORIGEN depletion calculation.

Three JMOCUP modules were specifically tailored for (1) the ATR driver fuel, (2) the compacts, and (3) the hafnium shroud and borated graphite holder. These three JMOCUP modules were set up to read the MCNP output-tally data, arithmetically manipulate the data, normalize it to the west lobe power, and finally write out the ORIGEN input files with updated cell power, cross sections, and isotopic masses. The JMOCUP script then executes the ORIGEN input files for the depletion calculation. When the ORIGEN depletion calculations are complete, the script executes three other JMOCUP modules that read the appropriate ORIGEN output files, manipulate the data, and write an MCNP scratch file updated with the new total number densities for the depletion-cell cards and new isotopic concentrations or number densities for the depletion-cell material cards. A seventh module reads the MCNP scratch file, calculates the new OSCC positions, determines if a neck shim rod has been withdrawn during this time step, and finally writes out the new MCNP input file. The bash script then executes the new MCNP model (input file) and the cycle starts over with the next time step. The process is repeated until the script execution completes the last time step.

Although the basic functionality of the JMOCUP system is similar to the MOCUP system, the JMOCUP system provides greater flexibility for the user in that modules can be easily copied and modified for reactor-specific applications. New functional modules can readily be interfaced with existing modules and incorporated into the JMOCUP execution script. This gives the JMOCUP system a certain degree of added flexibility and the ability to be applied to a variety of steady-state and transient reactor problems for any reactor system.

Some of the more notable features of the JMOCUP depletion calculation and code system include:

- Full core simulation
- Fully automated execution
- Control-element movement (OSCC and neck shim)
- Criticality search
- Easy restart capability
- Input data use as-run ATR measured data
- MCNP KCODE transport calculation option
- Unlimited number of time steps, plus variable length time steps
- Multiple region depletions with different type and number of isotopes/nuclear reactions
- Any number of MCNP depletion cells in each region
- Decay of radionuclides between ATR power cycles with variable shutdown times between cycles
- High resolution depletion calculation
- Computer-intensive calculation.

The JMOCUP methodology and base modules have been applied previously to several different nuclear reactors for spent-fuel isotopic predictions and reactor core designs [10]–[15], and to an actual measured reactor power maneuver or transient analysis with variable-length time steps. In this transient case, a power up-down-up maneuver was used to measure the reactor’s power coefficient of reactivity. The core k-effective was calculated at each time step, where the time-step lengths varied over a range of just a few seconds to up to several minutes. Very short time steps were necessary to simulate the rapid control-rod movements and the resulting measured core power changes and xenon concentration changes during the power-down and the power-up segments of the transient. Longer time steps (few minutes) were used before and after the power maneuver and during the steady-state power conditions. The transient calculation produced estimates of the core k-effective and reactivity changes while accounting for the time-dependent behavior of important isotopes such as Xe-135 during the transient.

In the JMOCUP methodology, the neutron-transport problem is solved using the KCODE option in the MCNP code. For the KCODE option to be effective, the reactor core, in this case the ATR driver fuel, must be simultaneously depleted along with the AGR-2 experiment depletions. Depleting the ATR driver core provides an excellent irradiation neutron source or neutron starting distribution for the AGR-2 experiment exposure. However, depleting the full ATR core comes with a price, namely, (1) significant computer runtime to execute the massive MCNP model at each time step using the KCODE option, and to calculate the large amount of tally data required for the JMOCUP depletion calculation, (2) the need to load the ATR driver core at the beginning of each power cycle with the appropriate 40-element loading placed in the correct serpentine-core positions, (3) depletion of 840 extra ATR driver core cells in the MCNP model at each time step, (4) the need to move the 16 OSCC drums and the 24 neck shim rods at each time step to maintain a near critical condition (k-effective ≈ 1.00), and finally, the need to model experiments in the flux traps to balance core reactivity and reproduce the actual ATR lobe power splits. Each of these issues costs either computer runtime or problem set-up time prior to the start of the depletion calculation. However, none of these issues, either individually or in combination, defeats the use of the KCODE option and, hence, the possibility of a full core high-resolution depletion calculation. Nevertheless, the result is a full core simulation with the best possible neutron source distribution for ATR experiment irradiations.

The JMOCUP modules are linked by a bash shell script, which is relatively easy to modify to accommodate additional modules. Additional modules can be added to increase the sophistication of the depletion calculation, (for example, changing MCNP cell material properties [density, temperature] at each time step, changing temperature-dependent cross sections at given time steps for cases involving variable experimental conditions, searching for the control rod position or a burnable poison concentration for criticality, or using super-fine time steps to simulate a reactor power maneuver or transient in which the control rods move on the order of seconds or less). Many of these additional features have previously been implemented with the specific JMOCUP modules for different reactor problems and applications.

One powerful feature of the Monte Carlo depletion technique is the use of continuous energy cross sections (MCNP) to solve the neutron-transport problem. Continuous energy cross sections eliminate the need for energy and spatial weighting of group cross sections needed in deterministic code transport calculations. Another powerful feature is the MCNP three-dimensional geometry capability that can essentially model any reactor system in explicit detail. The main drawback of Monte Carlo depletion calculations is, of course, the relatively longer runtimes to solve the neutron transport problem. This is particularly true in the case of the KCODE option in MCNP5 and the very large ATR MCNP models.

6.1 ATR Measured Data

For each ATR power cycle, ATR measured data or minutely as-run data, is taken directly from the ATR ASUDAS system and fed directly into the NDMAS system. NDMAS then averages the data over 1-hour or 24-hour time periods. The daily-averaged data is downloaded from the NDMAS system and formatted for use in the JMOCUP modules. The 24-hour averaged data or daily average data is then used in the daily JMOCUP depletion calculations. At the start of each JMOCUP depletion calculation, the as-run data must be loaded into the appropriate JMOCUP modules prior to execution.

Required as-run hourly ATR includes: (1) total core power (MW), (2) lobe powers (MW) for the northwest (NW), northeast (NE), center (C), southwest (SW), and southeast (SE) lobes, (3) outer shim control cylinder (OSCC) position measurements in degrees, and (4) neck shim withdrawals. Table 3 shows an example of hourly as-run data for the total core power data at the start of Cycle 145A.

Table 3. Typical hourly total core power as-run ATR data for the beginning of Cycle 145A.

		N-16 Unconstrained (MW)					N-16 Constrained (MW)				
Time	**Date**	**NW**	**NE**	**C**	**SW**	**SE**	**NW**	**NE**	**C**	**SW**	**SE**
200	9/5/2009	0.00	0.00	0.00	0.00	0.00	0.00	0.00	0.00	0.00	0.00
300	9/5/2009	0.06	0.06	0.09	0.07	0.08	0.06	0.06	0.09	0.07	0.08
400	9/5/2009	0.55	0.55	0.87	0.71	0.71	0.55	0.55	0.87	0.71	0.71
500	9/5/2009	6.18	6.17	9.67	8.02	8.10	6.41	6.42	9.83	8.29	8.35
600	9/5/2009	6.14	6.15	9.58	7.85	8.45	6.36	6.39	9.73	8.10	8.69
700	9/5/2009	6.08	6.11	9.46	7.80	8.48	6.26	6.31	9.58	8.01	8.68
800	9/5/2009	6.09	6.07	9.27	7.81	8.54	6.17	6.16	9.33	7.91	8.63
900	9/5/2009	6.08	6.05	9.15	7.80	8.58	6.22	6.20	9.25	7.96	8.73
1000	9/5/2009	13.50	13.49	20.20	17.42	18.98	13.29	13.27	20.06	17.18	18.76
1100	9/5/2009	13.46	13.43	19.72	17.11	18.65	13.26	13.21	19.58	16.87	18.44
1200	9/5/2009	16.14	16.17	23.35	20.57	22.29	15.77	15.77	23.10	20.15	21.89
1300	9/5/2009	16.20	16.23	23.08	20.69	22.40	15.73	15.71	22.74	20.13	21.89
1400	9/5/2009	16.80	16.81	23.50	21.42	23.04	16.22	16.18	23.09	20.74	22.42
1500	9/5/2009	16.97	17.01	23.33	21.61	23.00	16.41	16.41	22.94	20.96	22.40
1600	9/5/2009	17.00	16.96	23.02	21.54	23.13	16.39	16.30	22.59	20.84	22.48
1700	9/5/2009	17.09	17.06	22.92	21.57	23.06	16.49	16.41	22.50	20.87	22.41
1800	9/5/2009	17.10	17.10	22.79	21.73	23.20	16.51	16.45	22.37	21.04	22.55

A fifth piece of as-run data is needed in the set up of the ATR JMOCUP depletion calculation. This is the ATR core driver fuel-element loadings at beginning of cycle. These data include the U-235 and B-10 estimates of the mass loadings for each element, and are obtained from the ATR technical operations staff in the documented form of an ECAR. In addition, these reports identify the fuel element type and designated location in the core, and whether the elements are fresh or previously burned. For the AGR-2 JMOCUP calculation, all cycle ECARs used in the JMOCUP depletion calculation are listed in Section 2.0. These element loadings are put into a FORTRAN computer program that appropriately distributes the uranium and boron-10 to the 21 cells composing each ATR element and writes out a material card for each cell. These data are then loaded into the MCNP model by the user.

Note that the logic and functionality of the JMOCUP modules do not change from cycle to cycle; only the as-run cycle data (input data) loaded into each module change prior to execution.

6.2 Data Libraries

Standard MCNP cross-section data libraries (ENDF-7, ENDF-6, and ENDF-5) were used in the AGR-2 JMOCUP depletion calculation. The DOPPLER and NJOY codes were also used to generate temperature-dependent cross sections for the AGR-2 compact actinides using the standard room-temperature libraries. These cross-section data libraries are the same ones generated and used in the

AGR-1 JMOCUP depletion calculations. The ORIGEN2 base library was the PWRU.LIB that comes with the RSICC standard issue of the ORIGEN code.

7. ANALYSIS AND CALCULATIONS

MCNP output tally results are reported in the MCNP output on a per source-neutron basis. All fission power, heat-rate, flux, and reaction-rate tallies must be normalized to the ATR total core power or the ATR lobe powers. In the JMOCUP calculation, the ATR depletion calculation is normalized to the total core power, and the AGR-2 depletions are normalized to the west flux trap power, which is approximated as the average of the NW, C, and SW lobe powers (Section 2.0, Assumption 8).

8. SOFTWARE

The five computer codes (MCNP5, JMOCUP, ORIGEN2.2, DOPPLER, NJOY) used to perform this physics analysis are listed in Table 4.

Table 4. INL qualified analysis software version and record number.

Code Name	Version	V&V Record/ Document	Computer System	Operating System Software
MCNP	5 (Release 1.60)	PLN-4099	quark	SUSE Linux Enterprise Server Version 11.3
ORIGEN	2.2	PLN-3710	quark	SUSE Linux Enterprise Server Version 11.3
DOPPLER	0	Ref. [10]	PC (Prop. ID 418384)	Microsoft Windows
NJOY	99.0	Appendix C	quark	Open SUSE 11.3
JMOCUP	0	Appendix D	icestorm/quark	SUSE Linux Enterprise Server Version 11.3

MCNP5 and ORIGEN2.2 are listed under the INL Enterprise Architecture Repository and are qualified as scientific and engineering analysis software. MCNP has been verified for use on the INL fission, icestorm, and quark supercomputers by running the sample problems transmitted on the installation MCNP CD issued by the Radiation Safety Information Computational Center (RSICC) and comparing the calculated results against the standard results provided on the CD. This verification process was performed for MCNP Version 5 (Release 1.60).

The DOPPLER code was obtained directly from R. E. MacFarlane (code author) and P. Talou at Los Alamos National Laboratory. An extensive verification of this code on the WINDOWS PC (418384) has previously been performed [10]. Development of the high-temperature cross sections for the AGR-1 JMOCUP depletion calculation used this same verified code, input files, and computer platform. DOPPLER input files from [10] were only slightly modified for the development of AGR-1 high-temperature cross-section libraries. The slight modifications involved only the change of the desired cross-section temperature and/or the starting room-temperature cross-section library.

The NJOY computer code software and nuclear data was obtained directly from the Radiation safety Information Computational Center (RSICC) under the code name NJOY99.0, software package P00480MNYCP00 and RSICC No.: PSR-480, and installed on the INL quark computer system.

9. JMOCUP VERIFICATION

The JMOCUP depletion calculation underwent a rigorous verification for the AGR-1 depletion calculation documented in [1]. The same JMOCUP modules are used for the AGR-2 calculation. JMOCUP verification for the AGR-1 test focused on three areas: (1) verification of the as-run ATR data into JMOCUP formatted data; (2) JMOCUP module functionality and execution performance and, because of the large amount of output data, data selection, and data extraction; and (3) data plotting of key physics parameters in order to assess the performance and accuracy of the JMOCUP depletion calculation. Appendix D [1] provides the verification documentation for the JMCOUP modules.

In addition, the JMOCUP modules have previously undergone an extensive technical and functional verification [10] as well.

9.1 ATR Measured Data

The as-run ATR data (Section 6.1) are downloaded directly from the NDMAS database system and used directly in the JMOCUP modules with only minimal reformatting.

9.2 JMOCUP Module Functionality

An extensive verification of the functionality of the JMOCUP modules was performed previously [1]. A limited verification of the JMOCUP module functionality was again performed for the AGR-2 calculation by checking the input and output of the JMOCUP modules. Calculated MCNP flux and reaction rates, conversion to cross sections, placement of the cross sections into the appropriate ORIGEN inputs, extraction of the ORIGEN output data, conversion to number densities, and placement back into the new MCNP input file were checked for the ATR core depletion, the AGR-2 compact depletion, the hafnium shroud depletion, and the borated graphite holder depletion.

9.3 Key Calculated Physics Parameters

The JMOCUP depletion calculation for the AGR-2 test generated a significant number of output files with calculated results making it difficult, if not impossible to check each and every number. However, it is possible to plot key physics data to ensure that the JMOCUP depletion performed as expected and the calculated results are reasonable and well-behaved. This section will present calculated results of key parameters that provide additional verification for the JMOCUP calculation. Selected parameters include: (1) ATR uranium-235 depletion versus total ATR core power as a function of burnup (time step), (2) compact U-235 depletion as a function of burnup, (3) boron-10 depletion in the borated graphite holders as a function of burnup, (4) hafnium-isotope depletion and buildup as a function of burnup, and (5) calculated ATR core k-effective during a power cycle. Additional parameters are also evaluated in this section.

9.3.1 ATR Driver Fuel Depletion

Of the four JMOCUP depletions performed as part of the AGR-2 JMOCUP depletion calculation, the first depletion, or the depletion of the ATR driver fuel, was the largest in terms of the number of cells (840) to be depleted at each time step. One would expect the depletion of the uranium in the 840 driver cells to be directly proportional to the ATR total core power. And in particular, since the ATR driver fuel is high-enriched (93 wt%), the depletion of the total U-235 driver fuel mass should track the total ATR core power.

Figure 6 is a plot of the ATR U-235 depletion rate for Cycle 147A as a function of time step, plus the ATR total core power is plotted for comparison (red). It is evident that the amount of U-235 depleted in each time step tracks the ATR total core power very closely including the scram at time step 30. Figure 7 is an expanded view of the two curves in Figure 6 showing finer detail in the variation of the ATR U-235 mass depletion rate and the ATR total core power. Again, the two curves track very well, indicating the JMOCUP calculation depleted the ATR driver fuel elements as expected and in an accurate manner.

It should be noted that plots similar to Figures 6 and 7 were made for each of the other ATR power cycles for the AGR-2 test, and each exhibited the same excellent behavior. Although not shown here, additional plots of the total accumulated U-235 mass depleted as a function of time step for each power cycle also showed expected behavior with uniform, monotonically increasing curves; and plots of U-235 mass for individual depletion cells in each ATR element also showed well-behaved depletion behavior as well. It was concluded that the JMOCUP calculation performed the depletion of the ATR driver core in an expected and accurate manner.

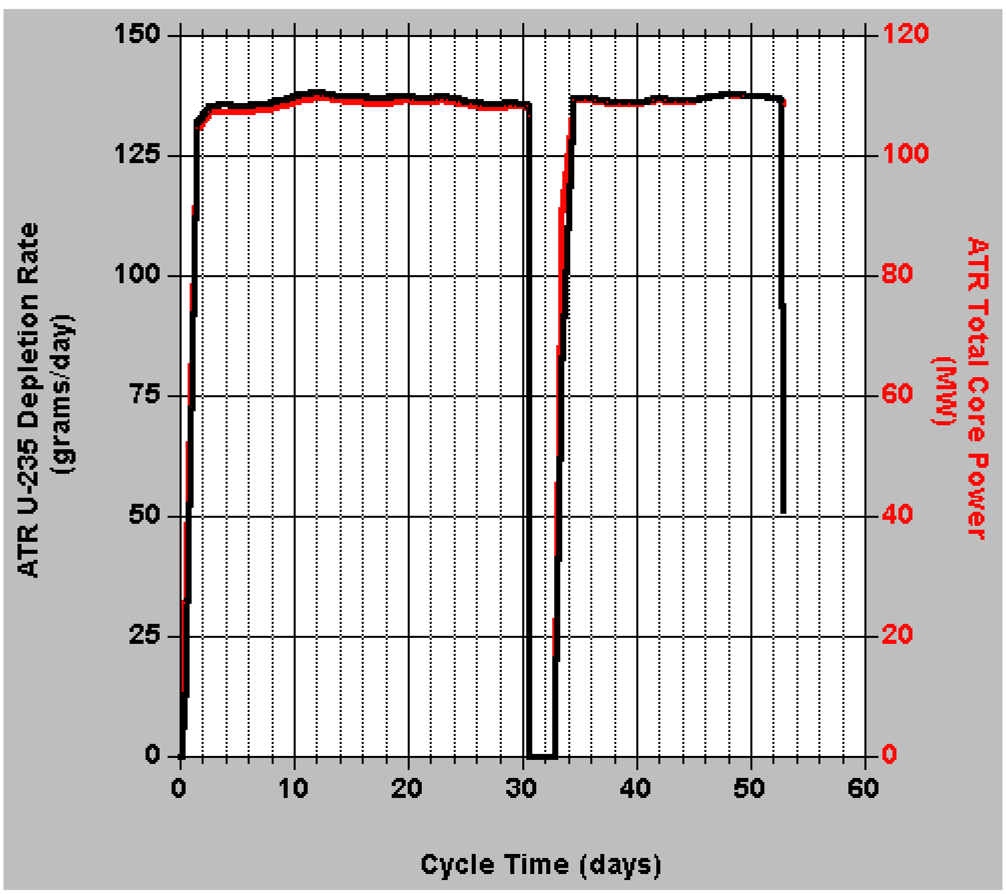

Figure 6. ATR driver fuel U-235 depletion rate and total ATR core power as a function of cycle time (Cycle 147A).

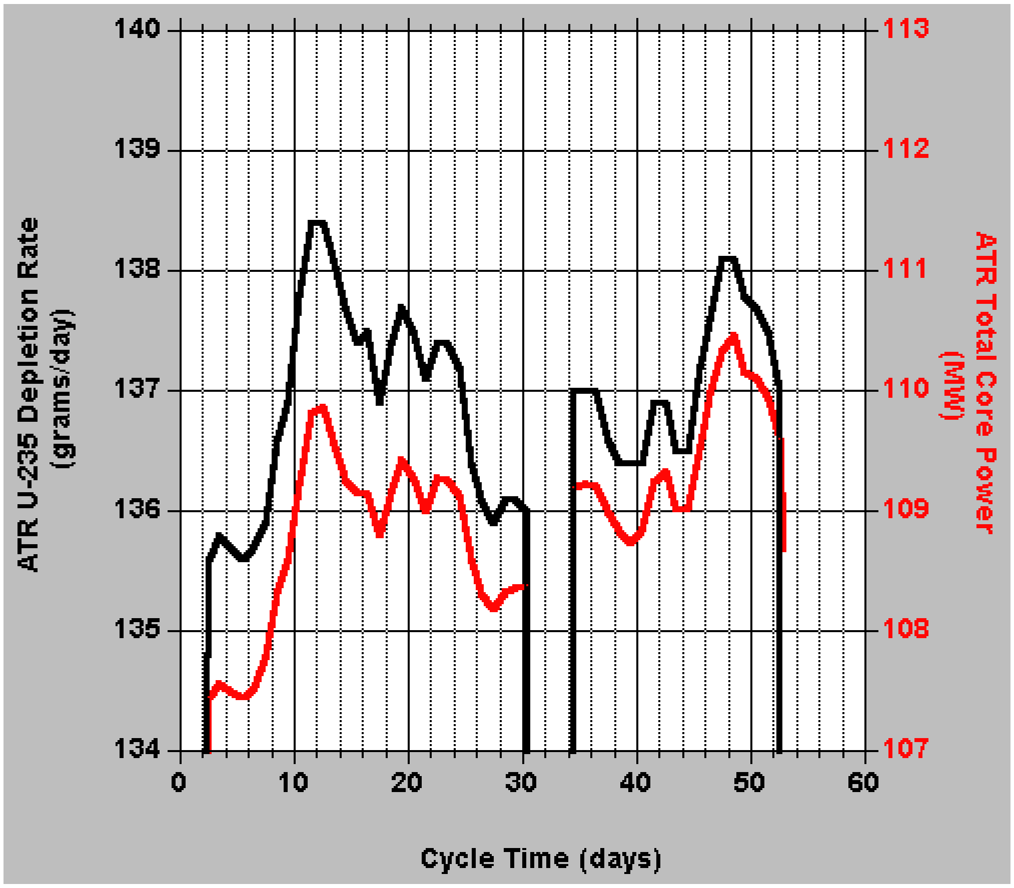

Figure 7. Expanded view of the same two curves in Figure 6 (Cycle 147A).

9.3.2 Compact Depletion

The second depletion performed by the JMOCUP calculation was the depletion of the 72 compacts in the six AGR-2 test capsules. Several important parameters were calculated for the compacts, including fission power, U-235 mass burnup, higher-order actinide isotopic mass, burnup in %FIMA, and fast-neutron fluence. These data will be presented in the results section.

Depletion of the compact U-235 mass was a good measure or indication that the JMOCUP depletion of the compacts performed the calculation as expected. Figure 8 shows the depletion of the total U-235 capsule mass as a function of the number of ATR power cycles. Extrapolation of the curve in this figure would indicate that after approximately 13 ATR power cycles the entire U-235 mass would be completely depleted. Since only eight cycles have been completed, an additional five ATR cycles of comparable length and power level would be required to achieve near total U-235 depletion. AGR-2 is projected to undergo five more cycles; however, one of these cycles will be of very short duration, so some small amount of U-235 is expected to remain at end-of-life or experiment conclusion.

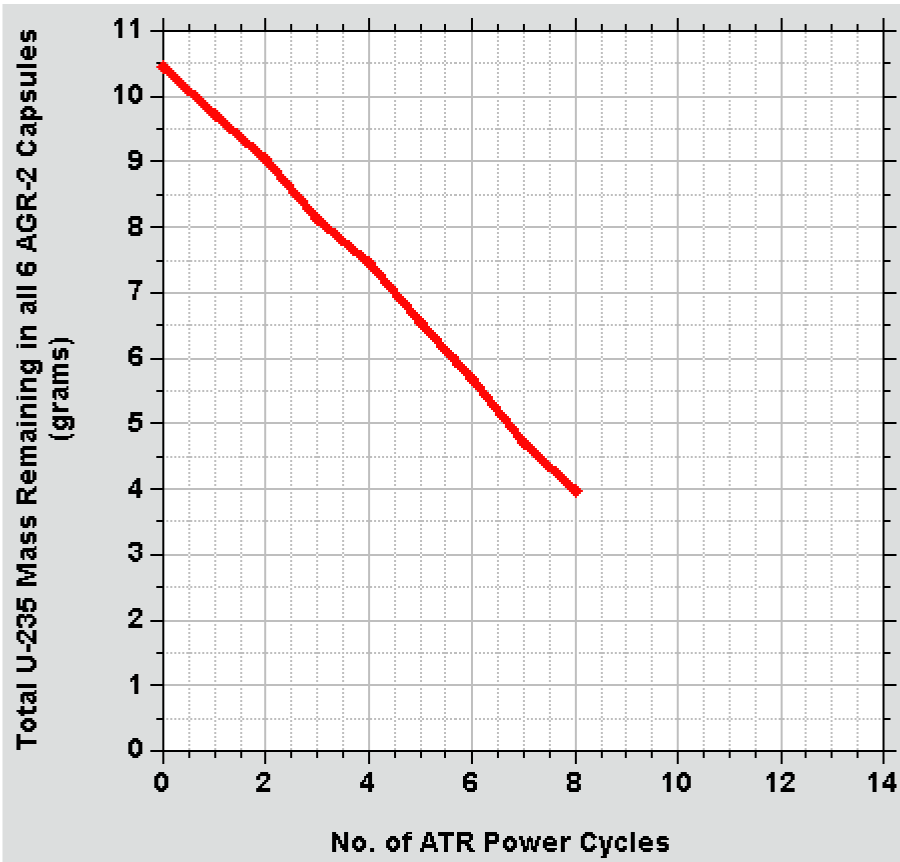

Figure 8. Depletion of the total U-235 mass in all six capsules as a function of the number of number of ATR power cycles.

9.3.3 Borated Graphite Holder Depletion

The third depletion performed by the JMOCUP calculation was the depletion of the 23 cells comprising the six borated graphite holders (four depletion cells for each graphite holder, except one, which arbitrarily had only three). Each of the six capsules had a borated graphite holder to provide structural support and configuration control of the compacts. The purpose of the boron-10 in the borated graphite holders was to reduce the thermal neutron flux intensity in the vicinity of the compacts, particularly during the first several ATR power cycles when the compacts were fresh. The boron-10 balanced the U-235 depletion rate in the compacts allowing thermal control (via helium-neon gas mix) to be maintained until EOL.

Figure 9 shows the total boron-10 concentration in all six borated graphite holders as a function of ATR power cycle. The boron-10 concentration at each cycle number on the x-axis corresponds to the beginning-of-cycle concentration. Depletion of the boron-10 in the holders was an important part of the JMOCUP depletion calculation. At beginning-of-life (ATR Cycle 147A), the total boron-10 mass in the six graphite holders was 1.834 grams. By the end of the seventh cycle (151A), most of the boron-10 is gone, and after the eighth cycle (151B), the boron-10 is virtually completely depleted. The boron-10 depletes uniformly and monotonically, as anticipated and, hence, adds confidence that the JMOCUP calculation performed as expected. It is also noted that the AGR-2 boron-10 depletion is very similar to the AGR-1 boron-10 depletion [1]. Table 5 lists the boron-10 mass in the individual 23 borated graphite cells in the MCNP model as a function of ATR power cycle.

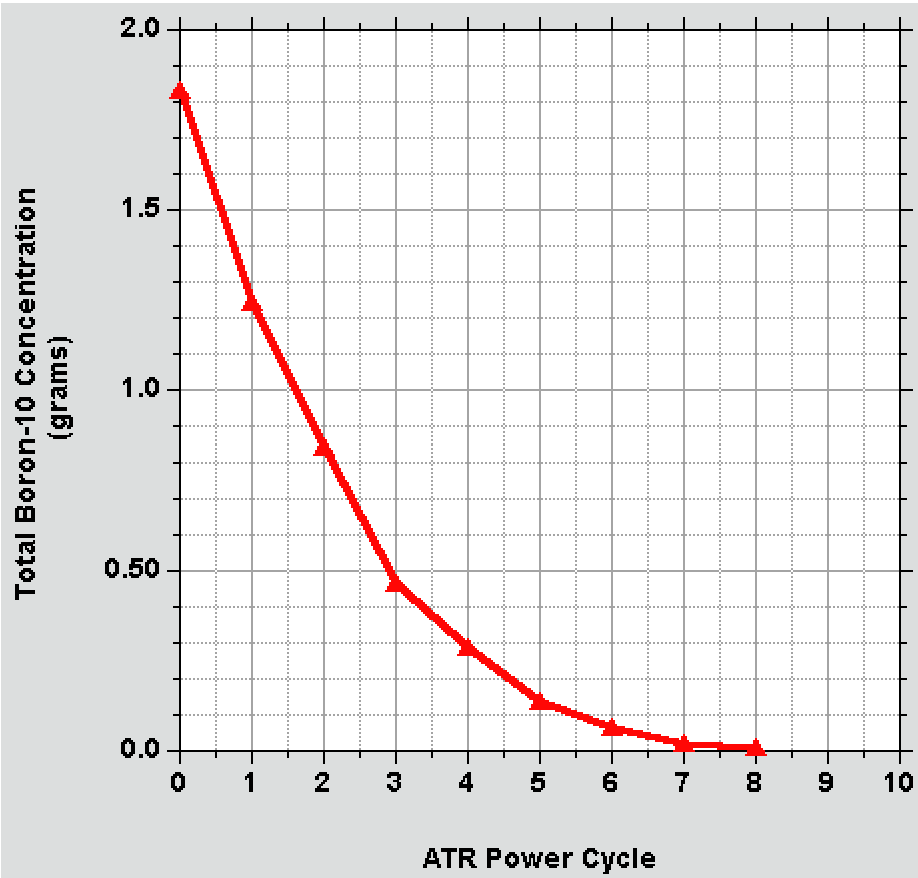

Figure 9. Total boron-10 mass in the six borated graphite holders.

Title: Preliminary JMOCUP As-Run Daily Depletion Calculation for the AGR-2 Experiment in ATR B-12 Position

ECAR No.: 2066 Rev. No.: 0 Project No.: 23843 Date: 10/09/2012

Table 5. Boron-10 concentration (grams) in each the borated graphite MCNP cell as a function of ATR power cycle after eight ATR cycles.

Capsule No.	MCNP Cell No.	147A BOC	148A BOC	148B BOC	149A BOC	149B BOC	150B BOC	151A BOC	151B BOC	151B EOC					
6	17169	3.443E-02	2.539E-02	1.918E-02	1.290E-02	9.485E-03	5.929E-03	3.635E-03	1.816E-03	9.510E-04					
6	17170	3.666E-02	2.830E-02	2.222E-02	1.571E-02	1.193E-02	7.728E-03	4.848E-03	2.456E-03	1.283E-03					
6	17171	7.382E-02	5.681E-02	4.442E-02	3.113E-02	2.340E-02	1.486E-02	9.079E-03	4.394E-03	2.194E-03					
6	17172	1.490E-01	1.086E-01	8.042E-02	5.187E-02	3.640E-02	2.086E-02	1.147E-02	4.860E-03	2.181E-03					
5	17173	8.500E-02	5.847E-02	4.045E-02	2.318E-02	1.456E-02	6.939E-03	3.127E-03	1.012E-03	3.642E-04					
5	17174	8.573E-02	6.126E-02	4.385E-02	2.626E-02	1.693E-02	8.232E-03	3.702E-03	1.166E-03	4.057E-04					
5	17175	1.303E-01	9.122E-02	6.368E-02	3.647E-02	2.255E-02	1.028E-02	4.348E-03	1.270E-03	4.172E-04					
5	17176	4.333E-02	2.716E-02	1.694E-02	8.255E-03	4.546E-03	1.806E-03	6.900E-04	1.834E-04	5.670E-05					
4	17177	7.264E-02	4.404E-02	2.615E-02	1.158E-02	5.857E-03	2.067E-03	7.120E-04	1.677E-04	4.757E-05					
4	17178	7.391E-02	4.786E-02	3.029E-02	1.455E-02	7.701E-03	2.816E-03	9.837E-04	2.319E-04	6.564E-05					
4	17179	7.389E-02	4.755E-02	2.982E-02	1.406E-02	7.316E-03	2.607E-03	8.870E-04	2.015E-04	5.542E-05					
4	17180	7.525E-02	4.554E-02	2.683E-02	1.165E-02	5.781E-03	1.981E-03	6.634E-04	1.498E-04	4.139E-05					
3	17181	7.271E-02	4.349E-02	2.519E-02	1.065E-02	5.183E-03	1.731E-03	5.679E-04	1.246E-04	3.382E-05					
3	17182	7.317E-02	4.700E-02	2.922E-02	1.353E-02	6.937E-03	2.416E-03	8.074E-04	1.781E-04	4.836E-05					
3	17183	7.434E-02	4.808E-02	3.012E-02	1.409E-02	7.281E-03	2.560E-03	8.615E-04	1.914E-04	5.229E-05					
3	17184	7.459E-02	4.535E-02	2.670E-02	1.151E-02	5.688E-03	1.927E-03	6.387E-04	1.413E-04	3.868E-05					
2	17185	8.448E-02	5.484E-02	3.486E-02	1.711E-02	9.395E-03	3.636E-03	1.344E-03	3.319E-04	9.857E-05					
2	17186	8.588E-02	6.016E-02	4.152E-02	2.303E-02	1.385E-02	5.965E-03	2.377E-03	6.300E-04	1.957E-04					
2	17187	8.651E-02	6.125E-02	4.279E-02	2.426E-02	1.487E-02	6.582E-03	2.692E-03	7.333E-04	2.326E-04					
2	17188	8.648E-02	5.853E-02	3.905E-02	2.075E-02	1.222E-02	5.190E-03	2.087E-03	5.704E-04	1.832E-04					
1	17189	6.454E-02	4.252E-02	2.778E-02	1.456E-02	8.691E-03	3.884E-03	1.703E-03	5.366E-04	1.957E-04					
1	17190	6.575E-02	4.680E-02	3.311E-02	1.945E-02	1.260E-02	6.254E-03	2.983E-03	1.026E-03	3.986E-04					
1	17191	1.319E-01	9.472E-02	6.795E-02	4.125E-02	2.765E-02	1.456E-02	7.426E-03	2.805E-03	1.179E-03					
	Sum	**1.834E+00**	**1.245E+00**	**8.426E-01**	**4.678E-01**	**2.908E-01**	**1.408E-01**	**6.763E-02**	**2.518E-02**	**1.072E-02**					

9.3.4 Hafnium Shroud Depletion

The fourth depletion performed by the JMOCUP calculation was the depletion of the hafnium shroud. The hafnium shroud was actually part of the stainless steel (SS316) test capsule wall; sandwiched between the thicker outer pressure vessel-containment steel wall and the thinner inner steel wall. The shroud itself was composed of six metal sheets, each a 60° arc section approximately 90 cm in length and 0.254 mm (0.01-inches) thick, formed together into an annular tube. Four of these 60° arc sections were hafnium metal, and two were SS316 steel. Figure 3 shows the hafnium (orange) and stainless steel (light blue) arc sections that comprise the neutron filter or hafnium shroud. The four 60° hafnium arc sections faced toward the ATR core center.

The purpose of the hafnium shroud was to balance the thermal flux and hence the compact stack powers. The two fuel compact stacks facing the core (Stacks 1 and 2) were shrouded by the hafnium to reduce their respective fission powers relative to the un-shrouded stack three furthest away from the core center. Whereas the boron-10 acts like a front-end burnable poison and depletes relatively rapidly during the initial ATR cycles, the hafnium shroud depletes at a relatively slower rate and maintains reduced levels of both the thermal and epithermal fluxes over the whole AGR-2 irradiation.

Natural hafnium is composed of six stable isotopes: Hf-174,176, 177, 178, 179, and 180. Of the six naturally occurring isotopes, Hf-177 has the largest thermal and epithermal radiative capture cross section, followed by Hf-174 and Hf-178. The other isotopes, Hf-176, Hf-179, and Hf-180 have relatively small capture cross sections. The natural abundances of the six hafnium isotopes are 0.162% (Hf-174), 5.206% (Hf-176), 18.606% (Hf-177), 27.297% (Hf-178), 13.629% (Hf-179), and 35.1% (Hf-180). Hence, the thermal neutron absorption by the shroud is dominated by Hf-177 and, to a lesser extent, by Hf-178. The small abundance of Hf-174 provides only a minor absorption effect.

Figure 10 shows the total hafnium shroud isotopic mass as a function of burnup or ATR power cycle, as predicted by the JMOCUP depletion calculation. One can clearly see how the Hf-177 depletes over time, because of its relatively large absorption cross section and small buildup contribution from Hf-176 transmutation. Similarly, Hf-174 mass noticeably depletes since it, too, has a substantial capture cross section and no transmutation buildup from lower hafnium isotopes.

Hafnium-178 remains relatively stable over the first power cycles (1–7) due to buildup from Hf-177 capture, but tends to decrease over time as Hf-177 depletes; Hf-178 continues to deplete due to its substantial capture cross section, which transmutes into Hf-179. Hf-179, as expected, simply continues to buildup in time from Hf-178 transmutation and minor depletion from its own relatively small capture cross section. Hf-180 mass remains relatively stable over the ATR cycles, balanced by Hf-179 transmutation and its own small capture cross section.

Therefore, depletion of the hafnium shroud isotopes behaves as one might expect, further building confidence that the AGR-2 JMOCUP calculation performed as expected. It is also noted that the AGR-2 hafnium shroud depletion is very similar to the AGR-1 hafnium shroud depletion [1].

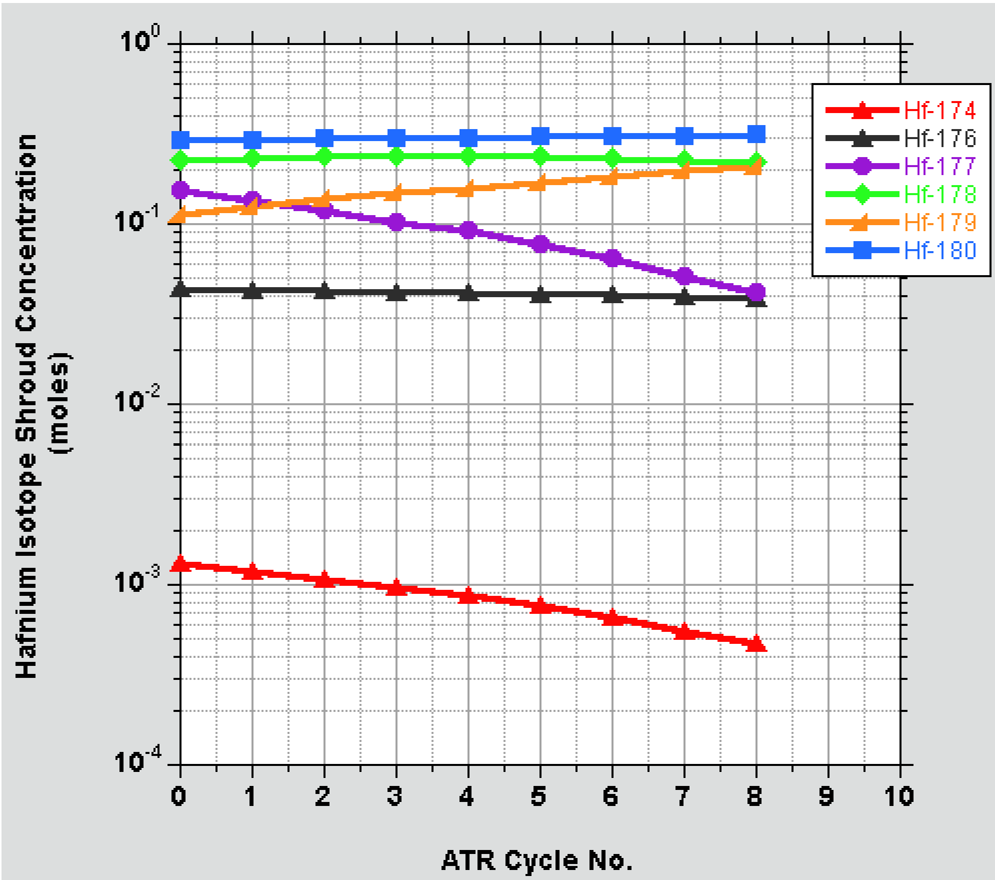

Figure 10. Total hafnium shroud isotopic mass as a function of the number of ATR power cycles.

9.3.5 ATR Core K-effective

An example of the JMOCUP-calculated core k-effective over an ATR power cycle (149A) is shown in Figure 11. Also plotted in this figure is the ATR total core power (red). The k-effective curve (black) exhibits very reasonable behavior by hovering around 1.00, or critical, as would be expected of a simulation of a critical reactor. The k-effective curve does experience a noticeable increase above 1.00 at BOC and is probably due to OSCC and neck shim adjustments as the reactor comes up in power. k-effective then remains relatively flat near 1.00 over most of the cycle, but then tends to increase slightly over the latter third of the cycle.

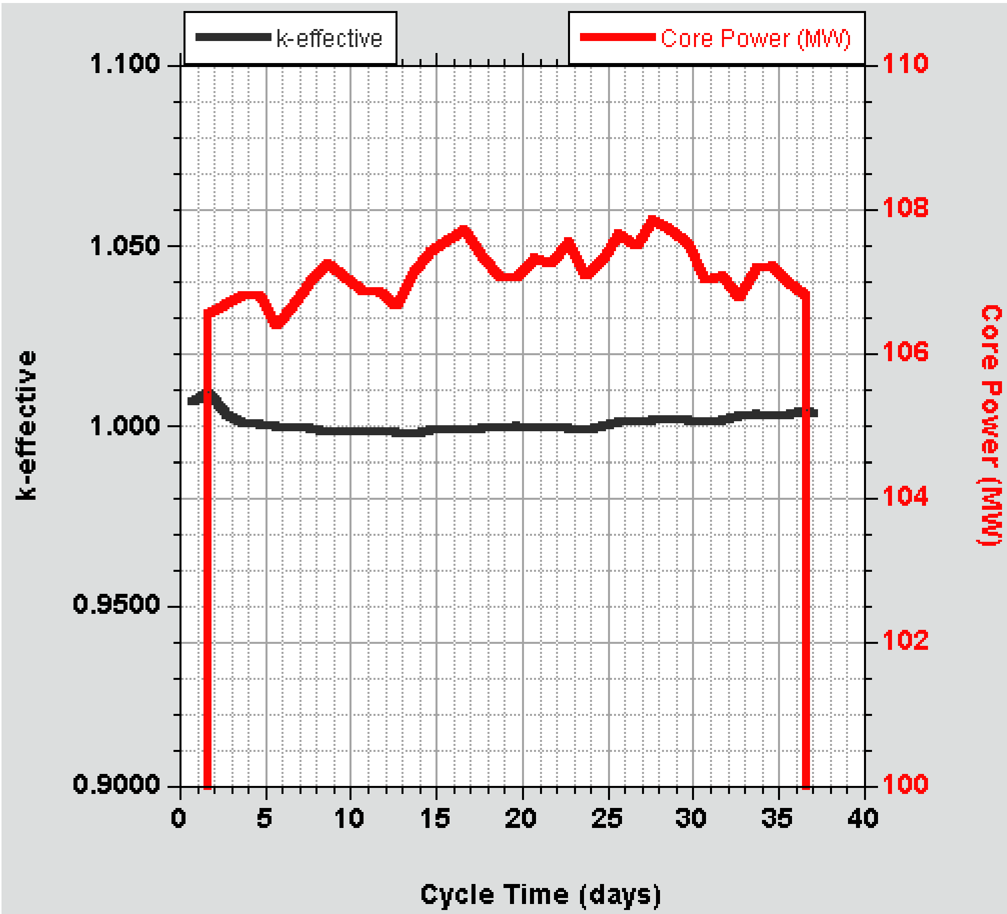

Figure 11. JMOCUP calculated k-effective for Cycle 149A.

This increase at the end of the cycle is not yet well understood, however, the following factors may contribute to this behavior: (1) MCNP modeling of the OSCC plate, (2) accumulated depletion of the hafnium isotopes in the OSCC plates and hafnium shim rods, and (3) depletion of other ATR experiments near the B-12 test facility.

9.3.6 OSCC Rotation

One important feature of the JMOCUP calculation was the ability to rotate the OSCCs in the MCNP model at each time step thereby simulating the actual ATR reactor operation. In order to verify the OSCCs were rotated properly in the JMOCUP depletion calculations, the OSCCs in the MCNP models were plotted at different time steps and compared to the ATR ASUDAS measured data.

As an example, Figures 12 and 13 show the two northeast OSCCs (N4 and E1) at beginning and end of cycle, respectively, for the ATR Cycle 145A from the previous AGR-1 JMOCUP simulation. In these two figures, the N4 (top) and E1 (lower) OSCCs are the full, big, dark-blue circular regions with a smaller light-blue or gray circle in the middle and a bright-pink arc (bent plate) on the periphery of the dark-blue regions. These bright-pink arcs are the hafnium plates, and they rotate counterclockwise from BOC to EOC.

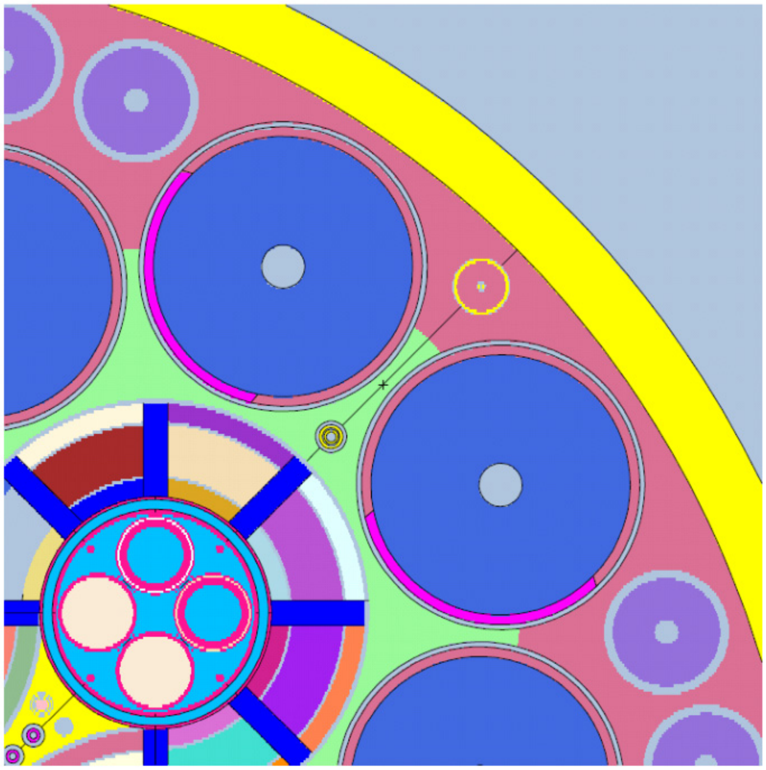

Figure 12. MCNP plot of the northeast (NE) OSCC at beginning-of-cycle for Cycle 145A showing the hafnium plate position on the N4 and E1 OSCCs (53.12°).

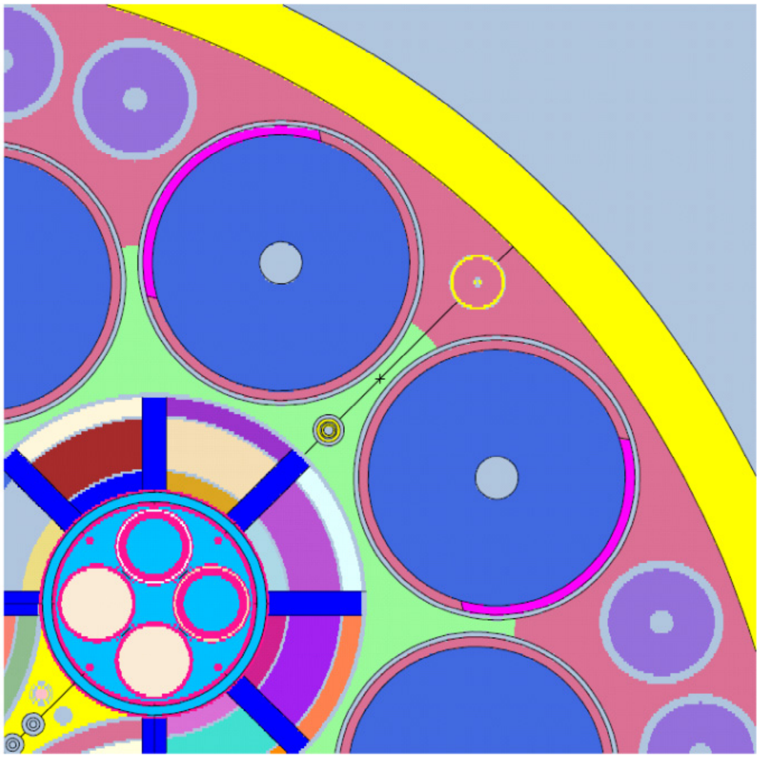

Figure 13. MCNP plot of the northeast (NE) OSCC at end-of-cycle for Cycle 145A showing the hafnium plate position on the N4 and E1 OSCCs (115.78°).

From the ATR ASUDAS data, the beginning-of-cycle position was 53.12 degrees (time step = 1) and the end-of-cycle position was 115.78 degrees (time step = 63). This is an angle change of 62.66 degrees. Using a protractor to measure the angular difference in the two MCNP plotted figures (Figures 12 and 13); the difference is estimated to be 63 degrees. These two values are in excellent agreement with one another, and one would conclude that the JMOCUP module performing the OSCC rotations is working properly. Note: the EOC 115.78-degree position is an example of a high-angle rotation position for an OSCC.

9.4 JMOCUP Validation

Partial validation of AGR-2 JMOCUP depletion calculation will be done through comparison with PIE data. Fuel compact end-of-life actinide and fission-product isotopic assay measurements and fast- and thermal-neutron flux wire measurements are expected to be the two primary data used to validate parts of the JMOCUP depletion calculation results.

The JMOCUP depletion methodology has also been previously validated for several different nuclear reactors and their assayed spent nuclear fuels [10]–[14].

10. DATA RETENTION

The number of input files and output files generated during the course of the AGR-2 JMOCUP depletion calculation is considerable. Storage of all of these files is prohibitive in terms of disk space, and some superfluous files have been deleted. Selected MCNP5 and ORIGEN2.2 files are stored on the

ICESTORM/QUARK hard-disk storage systems; in particular, those files associated with the AGR-2 fuel compacts have all been retained.

Post-processors that read, process, and output selected data from these input and output files are located on the ICESTORM and QUARK computer systems. All post-processed data will be downloaded to the INL nuclear data management and analysis system (NDMAS).

11. CALCULATED RESULTS

This section presents selected summary results for U.S. fuels calculated by the AGR-2 JMOCUP depletion calculation. The summary results are specifically for the TRISO particle compacts and include: (1) compact fission powers, (2) EOL %FIMA burnup, (3) EOL actinide isotopic concentrations, (4) EOL fission product concentrations, (5) EOL iodine-135 concentration, and (6) EOL neutron fast fluence. A complete inventory of these data and more will be available later in both later revisions of this ECAR and in the NDMAS at each ATR power cycle and timestep (daily) from the JMOCUP calculation.

In addition, results for the French and South African (S.A.) UO_2 fuels will be presented in later revisions.

11.1 Compact Fission Power

Compact fission power will be added in the next revision of this ECAR.

11.2 EOL %FIMA Burnup

Compact burnup (% FIMA) was calculated by the JMOCUP depletion calculation. Burnups were calculated for each compact or MCNP compact cell (one cell per compact) using the particle model. Compact average burnups (%FIMA) for all U.S. compacts are given in Table 6 for irradiation up to the end-of-cycle for cycle 151B (8^{th} power cycle). Figure 14 shows the Table 6 burnup data plotted as a function of compact number; Compact Number 1 is in Capsule 1 at the bottom of the capsule and bottom of the core; Compact Number 24 is in Capsule 6 (top of core) at the top of the capsule. There are three curves plotted, one for each of the three compact stacks. Since there are four compacts per capsule stack, there are four burnup values per capsule shown in the figure.

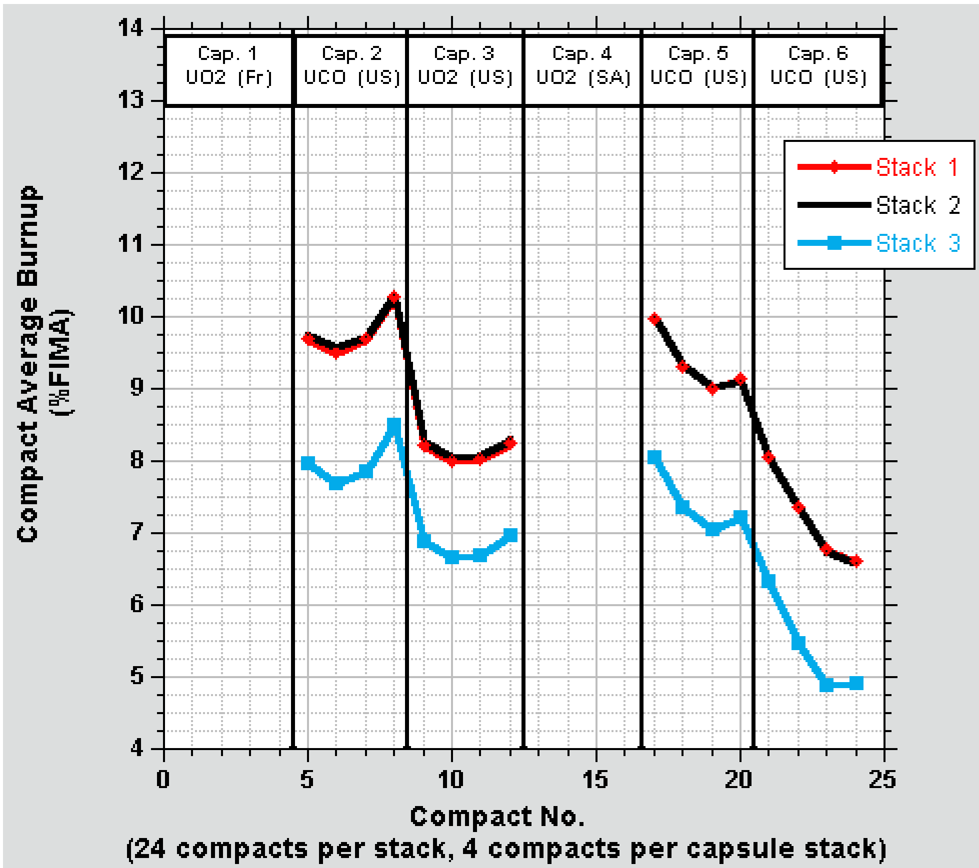

Figure 14. Calculated compact average burnups (%FIMA) by stack at the end of 8 ATR power cycle (EOC 151B).

There is some noticeable axial asymmetry in the burnup. Capsule 1 at the bottom of the core has the highest average burnups (not shown) and Capsule 6 the lowest at the top of the core. The stack burnups depend strongly on the capsule. These asymmetry capsule burnups are due to different TRISO particle characteristics in each capsule (particle uranium loadings, kernel size, and uranium enrichment) and the ATR chopped cosine axial power profile. It is also interesting to note the U-shaped burnup profiles of the compacts in each capsule. This was also observed in the AGR-1 test and is attributed to a slight increase in the thermal-neutron flux; therefore, the thermal fission compact power near the capsule ends because of the open-end design of the borated-graphite holders. The burnups in Stack 1 and 2 are nearly identical (Stack 2 burnups are slightly higher on average); both stacks face the ATR core center. Stack 3 has lower compact average burnups and is shadowed by Stacks 1 and 2. Stacks 1 and 2 have burnups ranging from approximately 6.5–10.25% FIMA, whereas Stack 3 burnups range from 5.0–8.5% FIMA.

Table 6. End-of-Cycle 151B compact average burnup in %FIMA.

Compact No.	Capsule No.	Level No.	Stack 1 (%FIMA)	Stack 2 (%FIMA)	Stack 3 (%FIMA)
24	6	4	6.61	6.60	4.90
23	6	3	6.78	6.76	4.89
22	6	2	7.37	7.37	5.47
21	6	1	8.06	8.06	6.33
20	5	4	9.13	9.10	7.22
19	5	3	9.01	9.03	7.06
18	5	2	9.30	9.33	7.35
17	5	1	9.96	10.01	8.06
16	4	4	--	--	--
15	4	3	--	--	--
14	4	2	--	--	--
13	4	1	--	--	--
12	3	4	8.26	8.32	6.96
11	3	3	8.03	8.10	6.70
10	3	2	8.00	8.06	6.65
9	3	1	8.22	8.28	6.89
8	2	4	10.29	10.30	8.50
7	2	3	9.70	9.72	7.87
6	2	2	9.51	9.57	7.69
5	2	1	9.68	9.75	7.97
4	1	4	--	--	--
3	1	3	--	--	--
2	1	2	--	--	--
1	1	1	--	--	--

Figure 15 shows Stack 2 compact average burnup (%FIMA) as a function of ATR power cycle. Each of the eight curves plotted represents the compact burnup achieved after the end of an ATR cycle. Each curve is for the same 24 compacts in Stack 2 in the six capsules. At BOL, the burnup is of course zero. With each cycle, starting with the first cycle (147A), the curves progressively increase in magnitude with the lower capsule compacts achieving slightly more burnup with each cycle causing a slight tilt in the curves from bottom to top capsule.

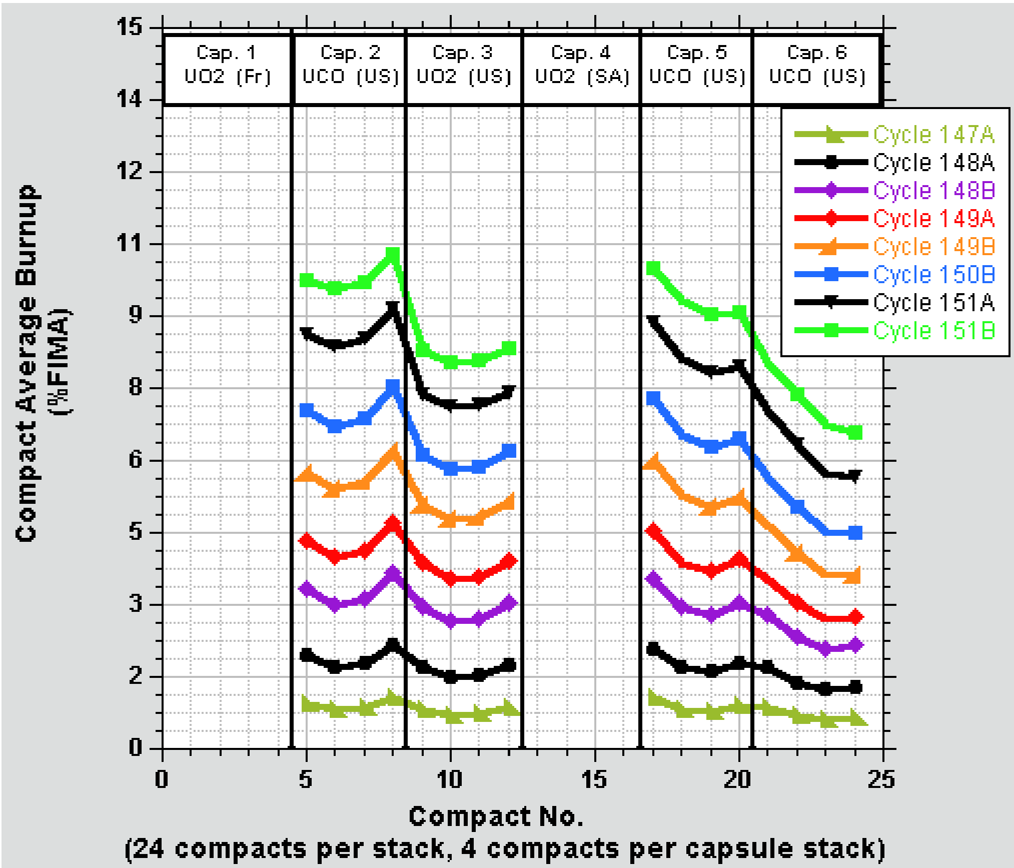

Figure 15. Calculated compact average burnups (%FIMA) as a function of ATR power cycle (Stack 2 only).

11.3 High-Burnup Compact Isotopic Fissions

This section presents specific burnup information for the highest burnup UCO (U.S.) compact after eight ATR power cycles. This highest burnup compact is Compact 2-4-2, or the compact in Capsule 2, Level 4, and Stack 2 (facing the ATR core). Compact 2-4-2 has a 10.3 %FIMA after eight cycles. Figure 16 shows the specific isotopic fissions as a function of JMOCUP time step (burnup) for this particular compact after the first eight ATR power cycles. Figure 17 is the same as Figure 16 except instead of JMOCUP time step; it is a function of burnup in units of GWD/MTU. One can calculate the absolute number of isotopic fissions by multiplying the specific fission value by 1.257 g U initial, where 1.257 g is the initial uranium mass loading for this high-burnup compact (UCO U.S.).

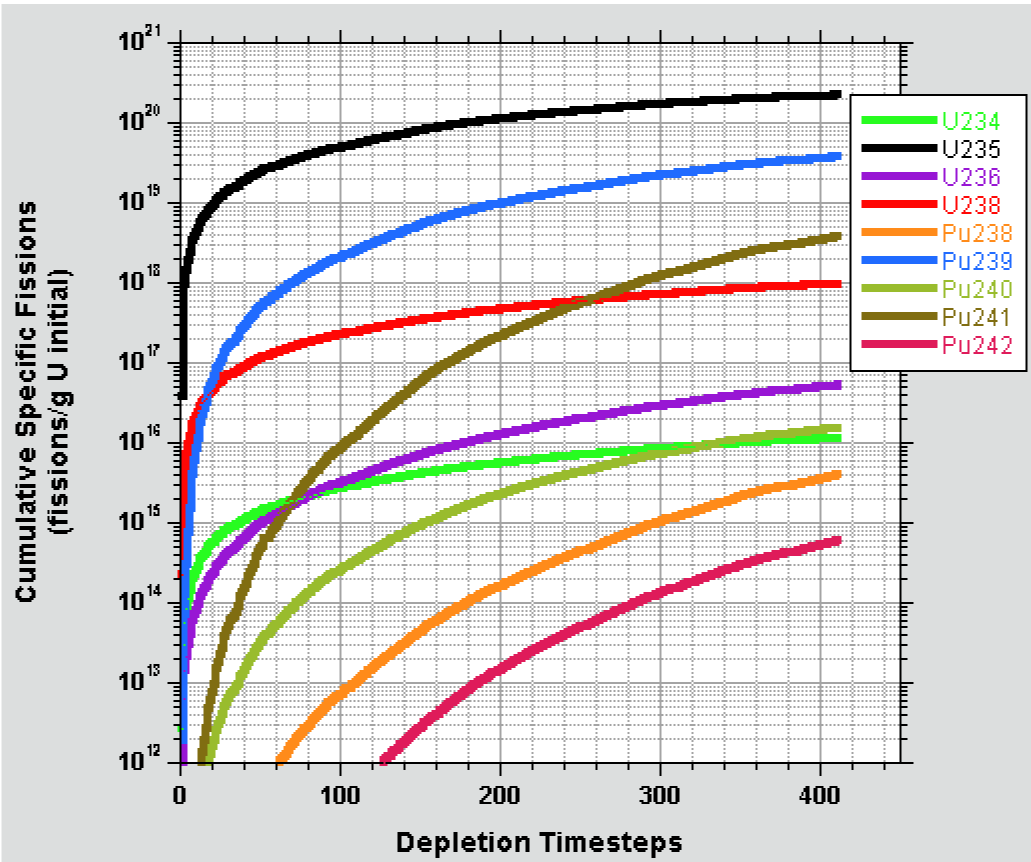

Figure 16. Isotopic cumulative specific fissions as a function of depletion timestep (burnup) for high-burnup compact 2-4-2 (UCO (U.S.)).

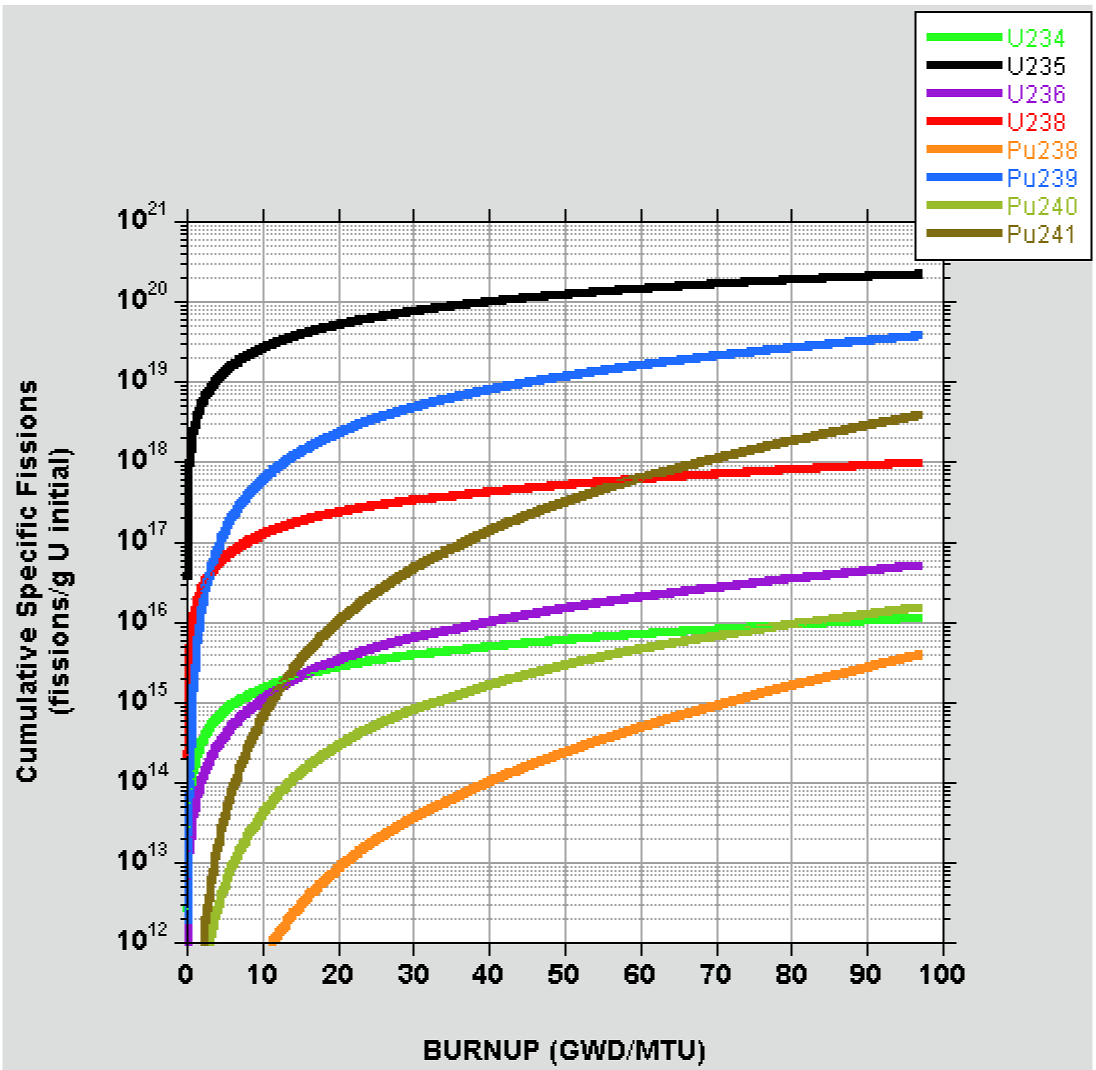

Figure 17. Isotopic cumulative specific fissions as a function of burnup (GWD/MTU) for high-burnup compact 2-4-2 (UCO U.S.).

Table 7 gives numerical values for the cumulative number of fissions (fissions/g U initial) at the end of each cycle as a function of burnup. Just the six major actinide isotopes are given. The right-hand column (green) totals the six isotopic fissions at the end of each cycle. The last row (red) gives the isotopic total after the current eight ATR power cycles.

Table 7. Cumulative EOC isotopic fissions (fissions/g U initial) by ATR cycle and burnup (Compact 2-4-2).

Cycle	Burnup (GWD/MTU)	U-235	U-236	U-238	Pu-239	Pu-240	Pu-241	TOTAL
147A	9.97	2.62E+19	1.08E+15	1.22E+17	5.80E+17	3.91E+13	6.42E+14	**2.62E+19**
148A	20.08	5.16E+19	3.42E+15	2.32E+17	2.29E+18	2.91E+14	1.04E+16	**5.16E+19**
148B	34.18	8.57E+19	7.75E+15	3.61E+17	6.01E+18	1.08E+15	7.71E+16	**8.58E+19**
149A	44.27	1.09E+20	1.21E+16	4.54E+17	9.42E+18	2.13E+15	2.00E+17	**1.09E+20**
149B	58.36	1.41E+20	1.98E+16	5.88E+17	1.52E+19	4.35E+15	5.61E+17	**1.42E+20**
150B	70.77	1.68E+20	2.78E+16	7.00E+17	2.13E+19	6.90E+15	1.14E+18	**1.69E+20**
151A	85.95	1.99E+20	4.00E+16	8.46E+17	2.99E+19	1.11E+16	2.37E+18	**2.01E+20**
151B	96.73	**2.19E+20**	**5.18E+16**	**9.68E+17**	**3.71E+19**	**1.53E+16**	**3.74E+18**	**2.23E+20**

After eight ATR power cycles (147A-151B), the isotopic fission fraction (% of total fissions) is given in Table 8.

Table 8. Isotopic fission fraction (%) at the end of the 8th ATR power cycle (Compact 2-4-2).

Isotope	Fission Percent (%)
U-234	0.0043
U-235	83.9299
U-236	0.0199
U-238	0.3710
Pu-238	0.0015
Pu-239	14.2318
Pu-240	0.0059
Pu-241	1.4356
Pu-242	0.0002

11.4 AGR-1, AGR-2, AGR-34, MHR, and PBMHR Physics Parameter Comparisons

This is a special section devoted to comparing plutonium fission fractions, heat rates, Ag and Pd production, PuFIMA, and neutron spectra as a function of burnup and enrichment for the AGR-1, AGR-2, AGR-34, MHR, and PBMR400. The MHR (prismatic modular helium reactor) and the PBMR400 (pebble-bed modular reactor) have previously been introduced in INL/TEV-1022, "Response to Questions about the Applicability of the AGR Test Results to NGNP Fuel" [19]. It should be noted that not all five experiments/reactors are included in every comparison due to availability of data.

Figure 18 compares plutonium fission fraction per gram of initial uranium as a function of burnup, where plutonium fission fraction is the total number of plutonium fissions from (Pu239 + Pu240 + Pu241) relative to the total number of fissions from (U235 + U236 + U238 + Pu239 + Pu240 + Pu241). The comparison is made between the AGR-1 and AGR-2 experiments, and the hypothetical modular helium reactor (MHR) fuel. The MHR curve (red) and the AGR-1 curve (black) are based on previously published results from INL/TEV-1022 [19]. The MHR fuel is assumed to have a single fissile particle with an enrichment of 19.9 wt%; AGR-1 fuel has similar 19.7 wt% enrichment. The parenthetical values for the AGR-1 and AGR-2 irradiation refer to specific compacts.

These results illustrate that the reduction in enrichment in the AGR-2 UCO (14.0%) and AGR-2 UO_2 (9.6%) relative to the AGR-1 fuel (19.7%), does increase the plutonium fission fraction in the fuel at a given burnup. As the enrichment decreases, there is less fission in U-235 and more absorption in U-238, which eventually results in Pu-239 production and fission. At low burnups (20-50 GWD/MTU) a higher fraction of fissions in the 9.6% enriched fuel are from plutonium than in the 19.9% TRISO fuel in the MHR at a similar burnup. At intermediate burnups, (~ 100 GWD/MTU) the 14.0% enriched AGR-2 results in a cumulative plutonium fission fraction that is closer to the MHR than the 19.7% enriched AGR-1 fuel.

As an additional point of information, Figure 18 shows the plutonium fission fraction as a function of burnup for the PBMR400 with 9.6 wt% U-235 TRISO particle fuel enrichment. The calculated PBMR data here agrees very well with the AGR-2 9.6 wt% curve (green). For example, at ~80 GWD/MTU, the PBMR plutonium fraction is ~26% and the AGR-2 ~24%.

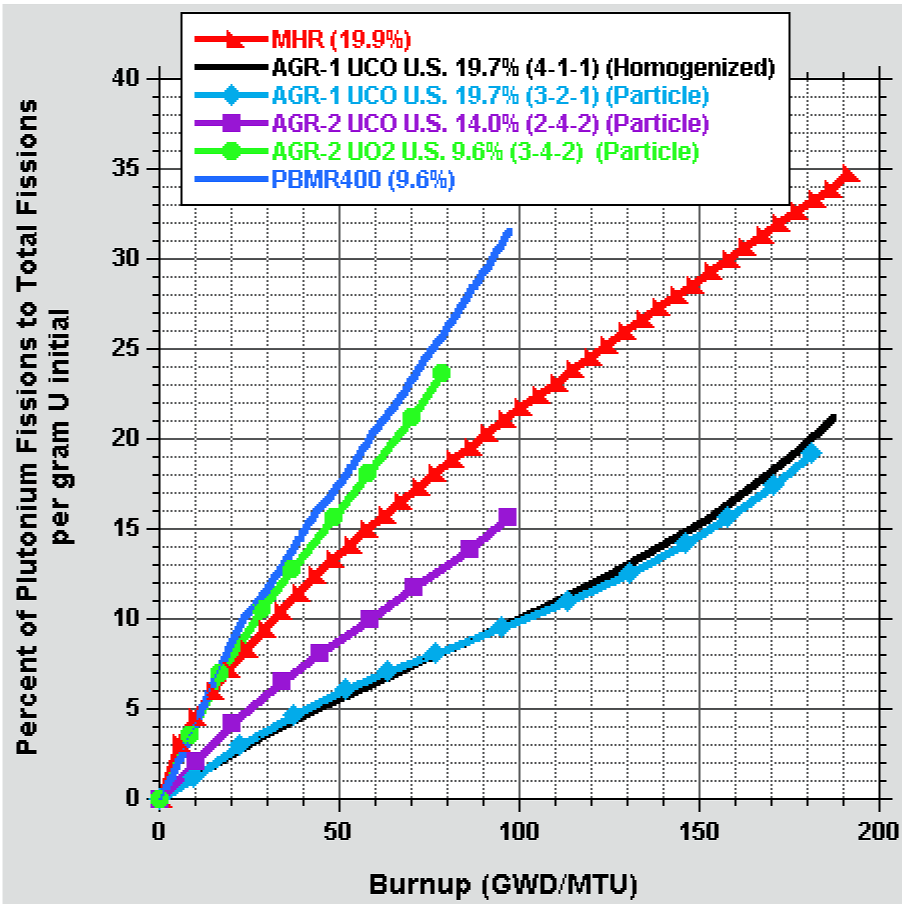

Figure 18. Comparison of plutonium fission fractions for different enrichment fuels from AGR-1, AGR-2, MHR [19], and PBMR400 [19].

Thus, while reducing the enrichment can increase the plutonium fission fraction to compensate for the differences in neutron spectrum between ATR and the MHR, it also has two other important impacts:

- The lower enrichments will limit the maximum burnup values that that can obtained in the ATR irradiation to well below the ultimate peak burnup for the MHR and still maintain the temperature in the irradiation
- The generation of Pd and Ag in the fuel is driven by two factors: fraction of fissions from plutonium (given the much higher fission yields of Pd and Ag from Pu than U) and the total number of fissions (i.e., burnup).

When these factors are considered together, while the plutonium fission fraction for the lower enriched AGR-2 fuel is closer to that expected in the MHR for a given burnup, the lower burnups that can be attained result in concentrations of Pd and Ag that are still less than the AGR-1 fuel.

Table 9 compares the cumulative production estimates for Ag and Pd for the five cases above at burnups around 100 GWD/MTU and at their peak burnups. Note that since the AGR-2 experiment is not yet complete, peak burnups have been projected to EOL along with the associate Ag and Pd concentration values. The cumulative production estimates for Ag and Pd are given in units of total atoms per gram initial uranium. Also included is the %PuFIMA value (percent plutonium fissions per initial metal atom).

Table 9. Comparison of Ag and Pd production versus burnup and enrichment.

Reactor/Expt.	Burnup (GWD/MTU)	Kernel Enrich. (wt%)	Ag (atoms/g U initial)	Pd (atoms/g U initial)	%PuFIMA
MHR*	95.5	19.9	9.39+17	1.27+19	2.14
MHR*	191.0	19.9	3.12+18*	3.74+19*	7.05
AGR-1* (4-1-1)	104.05	19.7	5.50+17	9.18+18	1.15
AGR-1* (4-1-1)	187.42	19.7	1.88+18*	2.51+19*	4.18
AGR-1 (3-2-1)	94.77	19.7	4.71+17	8.08+18	0.96
AGR-1 (3-2-1)	181.02	19.7	1.69+18	2.31+19	3.71
AGR-2 (2-4-2)	96.73	14.0	7.28+17	1.07+19	1.61
AGR-2 (2-4-2)	145.0	14.0	1.38+18	1.88+19	3.13
AGR-2 (3-4-2)	78.41	9.6	8.47+17	1.12+19	1.98
AGR-2 (3-4-2)	115.0	9.6	1.57+18	1.96+19	3.68

* *TEV-1022 [19]*

Red *values are linear extrapolation estimates based on AGR-2 projected EOL burnup.*

Despite the differences in peak burnups, the AGR-1 and AGR-2 Ag and Pd concentrations at peak burnups are very similar because of the similarities in the PuFIMA, but still lower than the MHR concentrations. It would be impractical to increase the Ag and Pd concentrations up to the MHR values through further reduction in enrichment. It is surmised that the borated graphite holders used to levelize power during the AGR-1 and AGR-2 experiments absorbed thermal neutrons that could have transmuted more U-238 and thereby inhibited the production of Pu-239 in the compacts. The AGR-3/4 experiment does not have borated graphite in the capsules and therefore may produce plutonium fission fractions and Ag and Pd concentrations closer to the MHR.

Figure 19 shows AGR-1 and AGR-2 compact heat rates (MW) as a function of burnup and parametrically as a function of enrichment. The 19.7, 14.0, and 9.6 wt% U235 enrichment compacts shown are AGR-1 compact (3-2-1) high burnup, AGR-2 compact (2-4-2) high burnup, and AGR-2 (3-4-2), respectively. The heat rates all tend to increase initially, reach a peak and then decline. It is noteworthy to point out the lower the enrichment, the lower the peak and the sooner the decline in heat compact heat rate which supports the above claim that even though lower enrichments may increase the plutonium fraction, maximum burnups will be limited and capsule temperature more difficult to maintain.

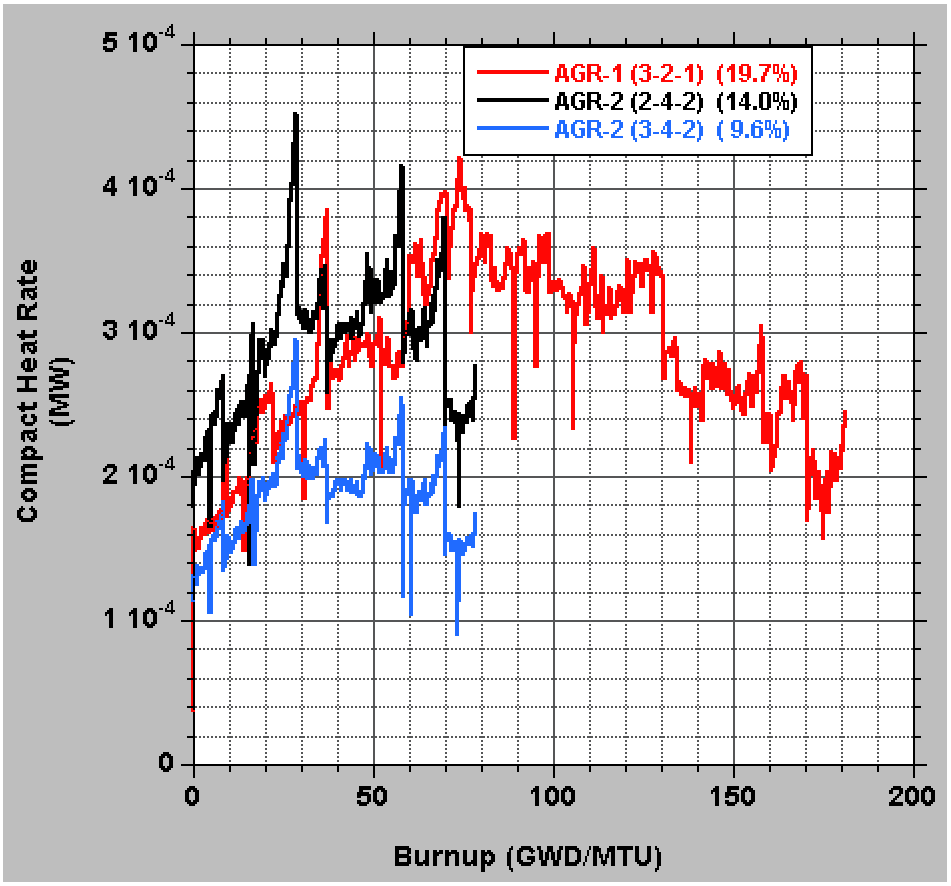

Figure 19. Compact heat rate comparison as a function of enrichment for three different compact enrichments from the AGR-1 and AGR-2 experiments.

Figure 20 compares neutron spectra between AGR-1 (BOL), AGR-1 (EOL), AGR-3/4 (BOL), and the MHR. With the exception of AGR-3/4, the spectra are all from the previously published INL/TEV-1022 [19]. The AGR-1 and AGR-34 fuels use 19.7-wt% enrichment and MHR assumes 19.9%.

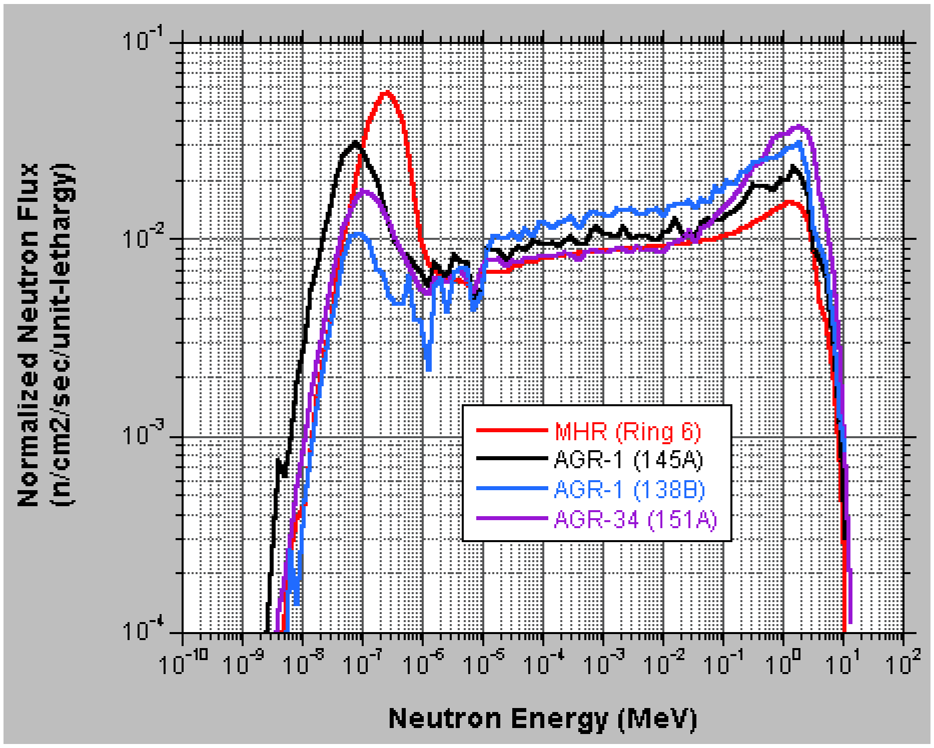

Figure 20. Neutron spectra comparison between the MHR, AGR-1, AGR-34, and MHR.

The two AGR-1 compact spectra in this figure are for BOL (138B) and EOL (145A). Comparing these two curves, the thermal neutron peak increases by a factor of three. Note that the other 11 AGR-1 cycle spectra between BOL and EOL have thermal peaks between the BOL and EOL peaks [19]. The AGR-1 boron-10 in the borated graphite holders burns out after approximately 7 cycles or ~100 GWD/MTU and increased thermal flux increases the rate of plutonium buildup. The upward curvature of the AGR-1 plutonium fission fraction curves (Figure 18) following boron-10 burnout can be explained by both the increasing plutonium concentrations in the compact and the depletion of U-235 (reduced fission rate after Cycle 141A).

The AGR-3/4 neutron spectrum (Figure 20) at BOL (Cycle 151A) has a thermal peak between the AGR-1 BOL and EOL spectra. There is no boron-10 in the AGR-3/4 capsule graphite to inhibit thermal neutron absorption by U-238 for the early cycles. Therefore, plutonium in the AGR-3/4 compacts should buildup at a faster rate and potentially has a greater plutonium fission fraction at EOL relative to the AGR-1 compacts. (Although not designed yet, this could also mean that AGR-5/6/7 could have plutonium fission fractions at EOL that are closer to an MHR. This will be examined as part of the AGR-5/6/7 design process.)

Also plotted in this figure is an average fuel spectrum for Ring 6 (inner fuel block annulus) in the MHR taken from INL/TEV-1022 [19]. The fuel temperature is assumed to be 1100°C and the block graphite 927°C. Figure 5 in INL/TEV-1022 [19] shows another spectrum for the MHR fuel and graphite at 20°C representing a bounding spectrum which has a thermal neutron peak lower by a factor of 2 and a shift in peak energy down to 0.08 eV (softer spectrum). Neutron spectra across the MHR active core are expected to lie between these two temperature-dependent curves, since the local spectra are strongly dominated by the bulk graphite/fuel temperatures.

11.5 EOL Actinide Isotopic Concentrations

This section presents the isotopic concentrations as a function of the number of ATR power cycles for the same high-burnup compact from the previous section, namely Compact 2-4-2, or the compact in Capsule 2, Level 4, and Stack 2 (facing the ATR core). Figure 21 shows the concentrations (moles) of the primary actinide isotopes in this compact at the end of each cycle. These same plotted data are also given in Table 10.

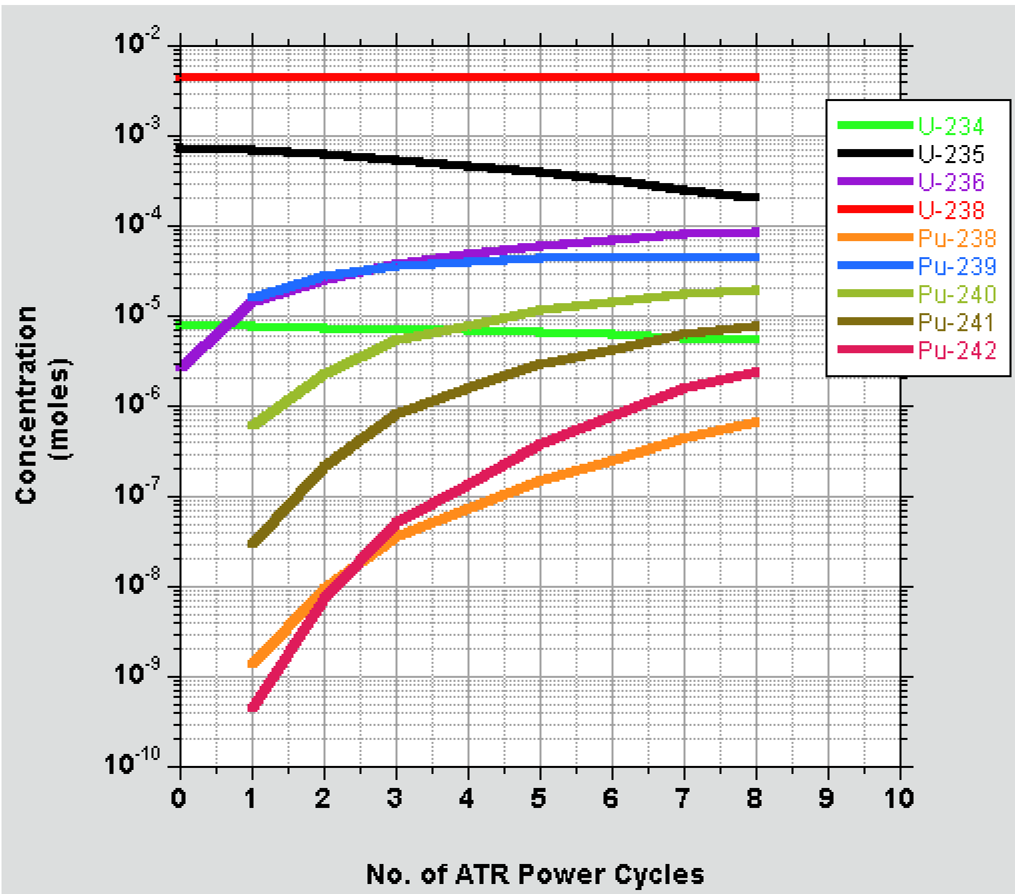

Figure 21. EOC 151B isotopic concentration as a function of the number of ATR power cycles for the high-burnup compact 2-4-2 (UCO U.S.).

Table 10. Isotopic concentrations (moles) at beginning-of-life and at the end of the 8th ATR power cycle (Compact 2-4-2).

Isotope	BOL (147A) (moles)	EOC (151B) (moles)
U-234	7.878E-06	5.502E-06
U-235	7.486E-04	2.049E-04
U-236	2.604E-06	8.801E-05
U-238	4.519E-03	4.356E-03
Pu-238	0.000E+00	6.522E-07
Pu-239	0.000E+00	4.426E-05
Pu-240	0.000E+00	1.968E-05
Pu-241	0.000E+00	7.860E-06
Pu-242	0.000E+00	2.433E-06

Initially, at beginning-of-life, or the start of Cycle 147A and the start of the JMOCUP depletion calculation, the single Compact 2-4-2 (high burnup) contained approximately 0.1760 g U-235 and 1.076 grams of U-238 and a total uranium mass of approximately 1.254 g U. This particular compact is a UCO (U.S.) type compact with an initial uranium enrichment of 14.029 wt% U-235. At the end-of-cycle (151B), or after the eight ATR irradiation cycles, Compact 2-4-2 contained after depletion 0.0482 g U-235 and approximately 1.0377 grams of U-238. This represents an average U-235 compact depletion of approximately 72.6%.

EOL compact actinide concentrations are given in Appendix A (*to be added in the next revision of this ECAR*) for each compact in units of moles/compact.

11.6 EOL Fission Product Isotopic Concentrations

In addition to the compact actinide concentrations, concentrations for the 71 tracked fission product isotopes are also given in Appendix B (*to be added in the next revision of this ECAR*) for each compact in units of moles/compact.

11.7 EOL Iodine-135 Concentration

(to be added at a later date)

11.8 EOL Neutron Fast Fluence

The fast fluence or cumulative fast flux (E_n > 0.18 MeV) has been calculated for each compact at every time step for each of the eight ATR power cycles so far. From these time-integrated fast fluxes, the corresponding compact cell fast fluence can be estimated. Table 11 is a summary of the cumulative compact fast fluence from BOC 147A through the EOC 151B, as calculated by the JMOCUP depletion calculation.

Table 11. AGR-2 compact fast fluence summary (E_n > 0.18 MeV) after only eight ATR cycles.

Capsule No.	Level No.	Stack No. 1 (n/m^2)	Stack No. 2 (n/m^2)	Stack No. 3 (n/m^2)
6	4	1.57E+25	1.57E+25	1.38E+25
6	3	1.72E+25	1.72E+25	1.51E+25
6	2	1.85E+25	1.86E+25	1.63E+25
6	1	1.95E+25	1.95E+25	1.72E+25
5	4	2.24E+25	2.25E+25	1.98E+25
5	3	2.35E+25	2.36E+25	2.07E+25
5	2	2.42E+25	2.43E+25	2.14E+25
5	1	2.45E+25	2.46E+25	2.17E+25
4	4	--	--	--
4	3	--	--	--
4	2	--	--	--
4	1	--	--	--
3	4	2.49E+25	2.51E+25	2.22E+25
3	3	2.50E+25	2.53E+25	2.23E+25
3	2	2.49E+25	2.52E+25	2.21E+25
3	1	2.45E+25	2.48E+25	2.18E+25
2	4	2.47E+25	2.50E+25	2.21E+25
2	3	2.46E+25	2.49E+25	2.19E+25
2	2	2.40E+25	2.43E+25	2.14E+25
2	1	2.31E+25	2.34E+25	2.06E+25
1	4	--	--	--
1	3	--	--	--
1	2	--	--	--
1	1	--	--	--

Capsule 6 is at the vertical top of the AGR-2 test train assembly (and top of the ATR core); Capsule 1 is at the bottom of the AGR-2 test train assembly.

11.9 Calculational Variable Uncertainties

There are uncertainties associated with the calculated JMOCUP depletion results. These uncertainties enter into the calculation from the ATR as-run data, ENDF cross-section data, MCNP statistical errors, etc. There are also unquantifiable propagation errors associated with Monte Carlo depletion calculations, although it has been shown that these errors tend to be well-behaved and average out over the depletion calculation. The high-resolution JMOCUP calculation is expected to behave very well and average out these propagation errors better than any other longer time step Monte Carlo calculation.

Table 12 lists potential variables in the JMOCUP calculation that might have an associated uncertainty. The uncertainties given in the table are estimates, and it is emphasized that they are only estimates, even though some uncertainties are more easily quantifiable than others.

Table 12. Variables and associated uncertainty estimates.

Entity/Item	Variable	Units	Uncertainty Estimate
ATR	Total core power	MW	±4.1%[17] ±8.0%[18]
ATR	Lobe power	MW	±4.1%[17] ±8.0%[18]
ATR	OSCC position	degrees (°)	<1.0%
ATR	OSCC hafnium isotope number densities	a/b/cm	<1.0%
ATR	Beryllium reflector poison		<1.0%
ATR	Flux trap reactivity		unknown
Fuel Compacts	BOL number densities	a/b/cm	±0.5%
JMOCUP-MCNP	k-effective		±0.5%
JMOCUP-MCNP	Flux (statistical error)	1/cm2/sn	±0.8%
JMOCUP-MCNP	Reaction rates (statistical error)	1/cm2/sn	±2.0%
JMOCUP-MCNP	Fission powers (statistical error)	MeV/gm/sn	±1.5%
JMOCUP-MCNP	ENDF nuclear data		0-10%
JMOCUP calc	Lobe power normalization	MW	+1-3%
JMOCUP calc	nu	n/fiss	±0.1%
JMOCUP calc	Q	MeV/fiss	±1.0%
JMOCUP-ORIGEN	Cross section	barns	±2.0%

JMOCUP-ORIGEN	Numerical error		±0.5%

The largest uncertainties listed in Table 12 are associated with the ATR total core power and lobe powers based on the cited references. The lobe powers and their summation, the total core power, are used in the JMOCUP calculation to normalize the neutron fluxes, reaction rates, and fission power densities. From the preliminary comparison of calculated compact FIMA and the measured FIMA, the excellent agreement between the calculated and measured burnups would indicate that the referenced uncertainty estimates for the ATR lobe powers and total core power are over estimated in magnitude. In fact, the measured ATR lobe powers and total core power estimates are instead probably quite good estimates and probably much more accurate than the quoted ±4%.

12. CONCLUSIONS

The JMOCUP depletion calculation for the AGR-2 TRISO coated fuel particle irradiation test has been completed for the first 8 ATR power cycles and appears to have executed successfully and accurately. The calculated depletion results for the AGR-2 JMOCUP calculation here match closely the calculated results from the AGR-1 JMOCUP calculation [1], specifically the ATR core depletion, the borated graphite holder depletion, and the hafnium shroud depletion. This was expected as both experiments and JMOCUP calculations were very similar in many respects. Also, the AGR-2 experiment placed in the ATR B-12 position is a mirror-image position to the AGR-1 B-10 test position. The AGR-2 depletion calculation does, however, exhibit more varied burnup results for the TRISO particle compacts, because of the four different types of TRISO particles in AGR-2 experiment versus the single TRISO particle type in AGR-1 experiment. The AGR-2 TRISO particle types differ in enrichment, kernel type, kernel density, kernel size, coating density and thickness, particle density, number of particles per compact. The burnup characteristics are also a strong function of the axial position in the test train assembly. Burnups for the U.S. AGR-2 compacts currently range from 4.9 to 10.3 %FIMA.

One important calculated physics parameter was the daily compact fission powers or heat rates (MW/cm^3) for each of the eight ATR power cycles. These data were calculated taking into account the daily ATR total and lobe power fluctuations, the OSCC rotational movement, and the periodic withdrawal of the hafnium neck shims. These compact heat rates were transmitted as input to the thermal calculation [16] for the prediction of the AGR-2 fuel and thermocouple temperatures.

In addition to the calculated compact fission powers, the JMOCUP depletion calculation provided additional calculated data as well. These additional data included compact (1) burnup (%FIMA), (2) thermal, epithermal, and fast fluxes, (3) fast fluence, (4) iodine-135 EOC concentrations, and (5) compact actinide and fission product concentrations. Other calculated depletion data (daily) from the JMOCUP calculation included: the ATR driver core, hafnium shroud, borated graphite holder, and ATR core k-effective.

The AGR-1 and AGR-2 JMOCUP depletion calculations have undergone rigorous technical checks and verification by independent technical checkers.

It should also be noted that the AGR-2 JMOCUP calculated %FIMA and fast fluence values are in good agreement with the AGR-2 design and pre-test physics depletion calculations and analysis [8].

13. REFERENCES

[1] ECAR-958, "JMOCUP As-Run Daily Depletion Calculation for the AGR-1 Experiment in the ATR B-10 Position," Revision 1, Idaho National Laboratory, August 2011.

[2] G. S. Chang and M. A. Lillo, "Thermal Neutron Flux Sensitivity Study for ATR Test Positions versus Outer Shim Control Cylinder Rotation," EDF-7326, Revision 0, Idaho National Laboratory, September 2006.

[3] B. Collin, "AGR-2 Irradiation Experiment Test Plan," PLN-3798, revision 1, Next Generation Nuclear Plant Project, Project No. 23841, Idaho National Laboratory, October 2011.

[4] X-5 Monte Carlo Team, *MCNP—A General Monte Carlo N-Particle Transport Code, Version 5*, Volume I (LA-UR-03-1987) and Volume II (LA-CP-03-0245), Los Alamos National Laboratory, Los Alamos, New Mexico, April 23, 2003.

[5] S. B. Ludwig and A. G. Croff, *ORIGEN2.2 – Isotope Generation and Depletion Code Matrix Exponential Method,* Oak Ridge National Laboratory, Oak Ridge, Tennessee (2002) and A.G. Croff, "ORIGEN2: A Versatile Computer Code for Calculating the Nuclide Compositions and Characteristics of Nuclear Materials, *Nuclear Technology*," Vol. 62, pp.335–352, 1983.

[6] R. S. Babcock, D. E. Wessol, C. A. Wemple, S. C. Mason, "The MOCUP Interface: A Coupled Monte Carlo/Depletion System," EG&G Idaho, Inc., Idaho National Engineering Laboratory, *1994 Topical Meeting on Advances in Reactor Physics*, Vol. III, Knoxville, Tennessee, Apri1 1–5, 1994.

[7] R. E. MacFarlane and P. Talou, "*DOPPLER: A Utility Code for Preparing Customized Temperature-dependent Cross Section Libraries for the MCNP Monte Carlo Transport Code*," User Manual, October 3, 2003.

[8] G. S. Chang, "Reactor Physics Analysis for the AGR-2 Experiment Irradiated in the ATR B-12 Position," ECAR-949, Revision 1, Idaho National Laboratory, June 2010.

[9] R. E. MacFarlane, "NJOY99.0: Code System for Producing Pointwise and Multigroup Neutron and Photon Cross Sections from ENDF/B Data," Los Alamos National Laboratory, distributed by RSICC as PSR-480 NJPY99.0.

[10] J. W. Sterbentz, "Spent Nuclear Fuel Source Term Calculational Methodology used at the Idaho National Engineering and Environmental Laboratory", Embedded Topical meeting of DOE Spent Nuclear Fuel and Fissile Material Management," *American Nuclear Society Transactions*, San Diego, California, June 7, 2000.

[11] J. W. Sterbentz, "Uranium and Plutonium Isotopic Validation Study for the Hanford N-Reactor," INEEL/EXT-02-01567, Idaho National Engineering and Environmental Laboratory, December 2002.

[12] J. W. Sterbentz, "Uranium Isotopics and Burnup Validation Study for the Fort Saint Vrain Reactor," INEEL/EXT-02-00861, Idaho National Engineering and Environmental Laboratory, November 2002.

[13] J. W. Sterbentz, "Validation Work to Support the Idaho National Engineering and Environmental Laboratory Calculational Burnup Methodology using the Shipping port Light Water Breeder Reactor (LWBR) Spent Fuel Assay Data," INEEL/EXT-99-00581, Idaho National Engineering and Environmental Laboratory, August 1999.

[14] J. W. Sterbentz, "Radionuclide Mass Inventory, Activity, Decay Heat, and Dose Rate Parametric Data for TRIGA Spent Nuclear Fuels," INEL-96/0483, Idaho National Engineering Laboratory, March 1997.

[15] J. W. Sterbentz, "INL MAPLE 1 Burnup-dependent Power Coefficients of Reactivity—Reactor Physics Analysis," INL/EXT-07-12516, Idaho National Laboratory, August 2007 (AECL proprietary).

[16] G. L. Hawkes, "AGR-2 Daily As-Run Thermal Analyses," ECAR-XXXX, Idaho National Laboratory, to be published.

[17] ATR-SAR-153, Chapter 4, Revision 13, Table 4.4-4 SINDA-SAMPLE statistical uncertainties.

[18] S. A. Atkinson and R. T. McCracken, "ATR Upgrade Final Safety Analysis Report," TRA-ATR-1211, Rev. 1, March 1997.

[19] TEV-1022, Rev. 1, "Response to Questions about the Applicability of the AGR Test Results to NGNP Fuel," Technical Evaluation Study, Idaho National Laboratory, September 27, 2010.

Title: Preliminary JMOCUP As-Run Daily Depletion Calculation for the AGR-2 Experiment in ATR B-12 Position

ECAR No.: 2066 Rev. No.: 0 Project No.: 23843 Date: 10/09/2012

Appendix A
EOL TRISO Particle Compact Actinide Concentrations

(data to be added following completion of the AGR-2 irradiation)

Appendix B
EOL TRISO Particle Compact Fission Product Concentrations

(data to be added following completion of the AGR-2 irradiation)

Appendix C
NJOY Cross-Section Data Verification

Traceability

The NJOY computer code was obtained from the Radiation Safety Information Computational Center as: ID: P00480MNYCP00, RSIC: PSR-480, Code Name: NJOY99.0. Applying patch updates created a new version of NJOY or NJOY99.161 on the Idaho National Laboratory (INL) HELIOS computer system.

Verification

To verify that the HELIOS NJOY code was generating ACER neutron cross sections properly, cross sections generated with the HELIOS NJOY code were compared to standard cross sections that are distributed with the MCNP computer codes. The standard cross sections issued by RSICC with the MCNP code are referred to as “RSICC 300K” in the following figures.

A comparison example is given in Figure C.1. This figure is a plot of the total cross section for U-235 at 300 K over the neutron energy range of 1.0E-11 to 20.0 MeV. Figure C.2 is the same as C.1, but only over the 1.0E-5 to 1.0E-3 MeV energy range showing more detail in the individual resonance behavior. Note that the red curves (NJOY HELIOS [300 K]) overlay the black curves (RSICC 300K) nearly identically, which is indicative of excellent agreement between the two cross section data sets and the fact that the HELIOS NJOY code is generating ACER cross-section data properly. The absorption, elastic scattering and fission cross sections are also in excellent agreement, although they are not shown here.

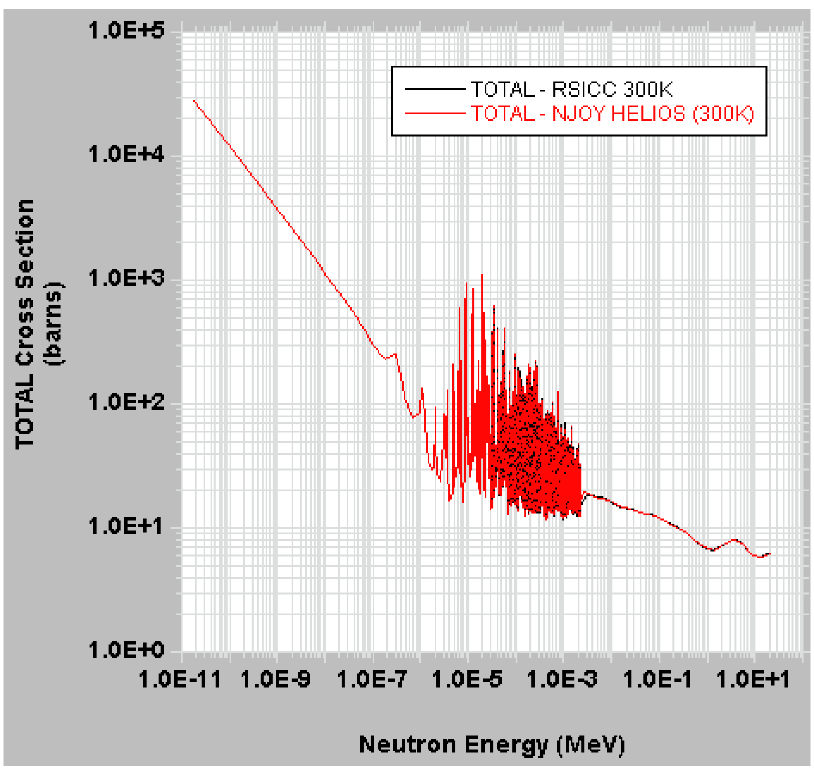

Figure C.1. Comparison of the U-235 TOTAL cross sections (300 K).

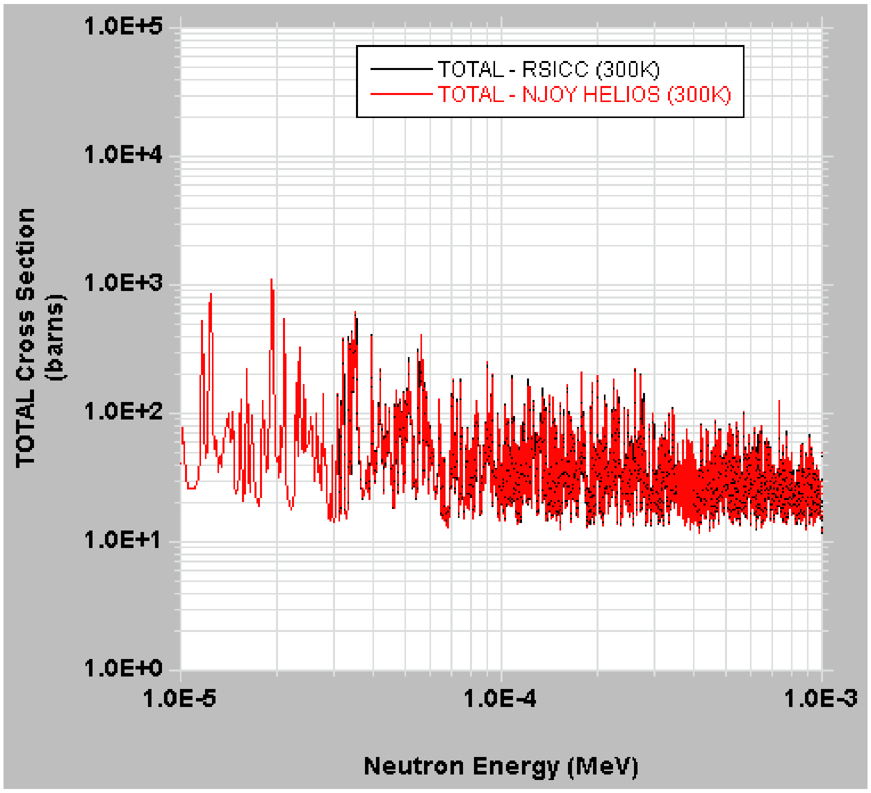

Figure C.2. Detailed comparison of the U-235 TOTAL cross sections (300 K).

As a second comparison example, Figure C.3 is a plot of the total cross section for the fission product Ag-110m at 300 K over the entire 1.0E-11 to 20.0 MeV energy range. Figure C.4 is the same as C.3, but only over the 2.0E-5 to 2.5E-5 MeV energy range showing a single resonance. Note that the red curves (NJOY HELIOS [300 K]) again overlay the black curves (RSICC 300K), which is also indicative of excellent agreement between the two cross-section data sets, and the fact that the HELIOS NJOY code is generating ACER cross section data properly.

The HELIOS NJOY code was also used to generate cross sections at temperature, namely 300 K, 600°C, and 1200°C. As an example to demonstrate that the HELIOS NJOY code properly Doppler-broadened the cross-section data, Figures C.5 and C.6 are presented for the total cross section (barns) of U-235 and Am-242m at 300 K, 600°C, and 1200°C, respectively. Doppler broadening of a single resonance, specifically for U-235, the resonance at 2.05E-6 MeV (2.05 eV) and for Am-242m, the resonance at 2.09E-6 MeV (2.09 eV) clearly show the desired broadening effect. Note that the 600°C and 1200°C cross-section library data was used in the AGR-1 JMOCUP depletion calculations for compacts. Specifically, the 600°C data was used for the first Cycle (138B), which was held at a relatively lower temperature, and the 1200°C data was used for the all subsequent ATR power cycles.

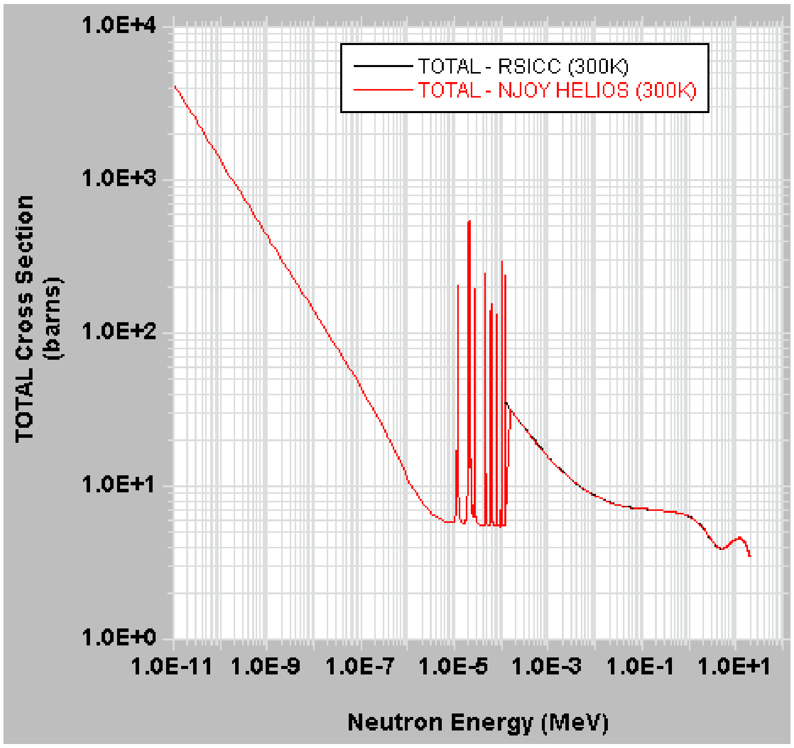

Figure C.3. Comparison of the Ag-110m Total cross sections (300 K).

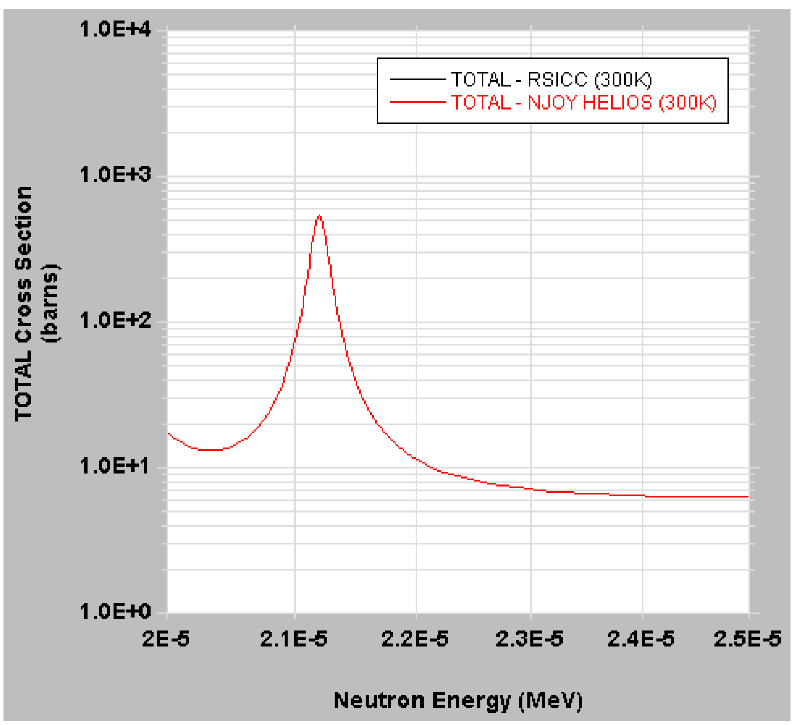

Figure C.4. Comparison of the Ag-110m TOTAL cross sections (300 K) for a single resonance.

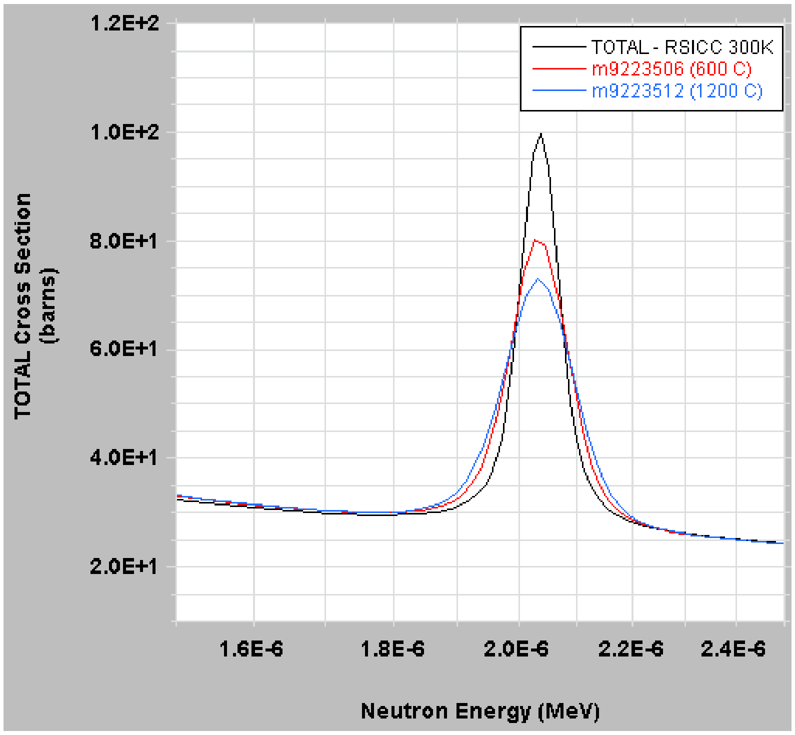

Figure C.5. Comparison of the U-235 TOTAL cross section at 300 K, 600°C and 1200°C for a single resonance.

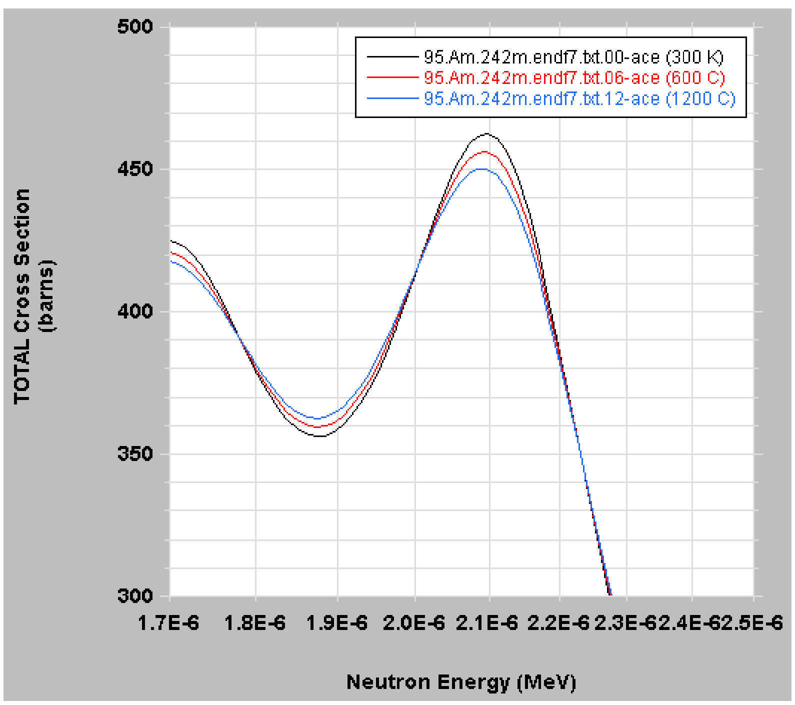

Figure C.6. Comparison of the Am-242m TOTAL cross section at 300 K, 600°C and 1200°C for a single resonance.

Title: Preliminary JMOCUP As-Run Daily Depletion Calculation for the AGR-2 Experiment in ATR B-12 Position

ECAR No.: 2066 Rev. No.: 0 Project No.: 23843 Date: 10/09/2012

Appendix D
JMOCUP Verification and Validation

AGR-2 Model Validation Inbox x

Sant, Robert L Aug 29

to me

Jim,

I completed my validation of the AGR-2 models. For this effort, the homogenized model (inp.1) and the particle model (inq.1) were compared to the data in the spreadsheet Reg.Blk.Enrich.AGR-2.2nd.calc.loading.b.xlsx (the spreadsheet had already been validated).

The following items were checked:

1. The homogenized model inp.1 was compared to the particle model inq.1. This included a comparison of all character/line differences between the models. Plots of the models were also viewed to accurate modeling of the compacts. Nothing unexpected was noted.

2. The arrangement of fuel compacts in inp.1 and inq.1 were correct (from bottom to top: French UO_2, US UCO, US UO_2, South African UO_2, US UCO, and US UCO).

3. The particle dimensions from the spreadsheet were compared particle model inq.1. All values were correct.

4. Plots of the particle model were used to validate the spreadsheet's "particles per compact". This showed that the number of particles per compact was not exactly replicated in the model (inq.1), but the modeled array was reasonable. For example, the particles per compact for the French UO_2 compact was 1,223.4, while the number of particles per compact in the model was 1,216. Likewise, the values for the US UCO compact are 3,171 vs 3,164, respectively. For the US UO_2 compact, the values are 1,555 vs 1,558, respectively. For the South African compact, the values are 1,512.2 vs 1,518, respectively.

5. The heights and diameters of the different compacts was not exactly replicated in the models. The compacts were all modeled with a height on 2.54 cm, while the actual compact heights varied from 2.5 to 2.52 cm. Likewise, all compacts were modeled with a radius of 0.617 cm, while the actual compact radii varied from 0.6125 to 0.6245 cm.

6. The number densities in the spreadsheet were compared to the particle model. A few of the total number densities were off in the last decimal place, but no other differences were noted.

7. The number densities in the spreadsheet were compared to the homogenized model. There were differences in the carbon, hydrogen, silicon, and total number densities for all of the compacts. For the French UO_2 compact, there were also differences in the uranium number densities. The values are shown below for the French UO_2 compact (material 8437).

Material	Spreadsheet	Model
O-16	1.28508E-03	1.285000E-03
C-12	7.24729E-02	7.214000E-02
Si-nat	1.51563E-03	1.515000E-03
U-234	1.35590E-06	2.896700E-16
U-235	1.27222E-04	1.272500E-04
U-236	1.98425E-06	3.754800E-12
U-238	5.11977E-04	5.153100E-04
Total	7.5916143E-02	7.558256E-02

8. After noting that some of the number densities in the homogenized model differed from the spreadsheet, a check of the total number densities was performed. In all instances, the values used in the model summed to the total number densities used in the model.

9. The tallies in the models were reviewed. No issues were identified.